5
Gas/Liquid Reactions

5.1
Micro Reactors for Gas/Liquid Reactions

5.1.1
Gas/Liquid Micro Flow Contactors

These devices have gas and liquid streams which do not merge, i.e. are not fed into each other. Rather, by use of separate ports both phases are passed in their own encasing, e.g. their own micro channel. Thereby, dispersion of the phases is prevented and only one large specific interface is created for mass transfer (different from dispersive micro devices, see, e.g., Section 5.1.2). The separate guidance of the phases allows to heat the phases separately, usually from the side most distant from the gas/liquid interface.

The advantage of the two-phase micro flow contacting concept is easy phase separation, as the phases are never inter-mixed. However, in view of the normally facile separation of gases and liquids, this is not of major impact. A real large benefit stems from operating with gas and liquid layers of defined geometry with a known, defined interface, unlike most disperse systems having a size distribution of their bubbles in the continuous liquid.

As a further advantage, the two-phase contacting approach facilitates having the same flow patterns when operating in many parallel micro channels. The key for proper numbering-up is flow equipartition. Since for the contacting approach only single-phase distribution is needed for both phases, it stands to reason that this is generally much more easily achieved as for multi-phase distribution given in dispersive mixers (see Section 5.1.2). Accordingly, numbering-up seems to be practicable for two-phase contactors and, indeed, existing falling film micro reactors already comprise an array of parallel-operated micro channels (see [R 1]).

The disadvantage of the two-phase contacting principle is related to the technical expenditure of realizing phase separation throughout the complete reactor passage. Special measures have to be taken to prevent phase inter-mixing. Also, this has to be controlled during the process. Hence inspection windows are essential (for the first prototype; they may be eliminated later).

Chemical Micro Process Engineering: Fundamentals, Modelling and Reactions
Volker Hessel, Steffen Hardt, Holger Löwe

ISBN: 3-527-30741-9

Figure 5.1 Photograph of a falling film micro reactor [1].

5.1.1.1 **Reactor 1 [R 1]: Falling Film Micro Reactor**

The falling film principle utilizes the wetting of a surface by a liquid stream, governed by gravity force, which thus spreads to form an expanded thin film.

The falling film micro reactor (Figure 5.1) transfers this well-known macro-scale concept to yield films of a few tens of micrometers thickness [1–3]. For this reason, the streams are guided through micro channels. To obtain a reasonable throughput, many micro channels are operated in parallel.

The liquid enters the micro channel device via a large bore that is connected to a micro channel plate via a slit (Figure 5.2). The slit acts as a flow restrictor and serves for equipartition of the many parallel streams [1, 3, 4]. The liquid streams are re-collected via another slit at the end of the micro structured plate and leave the device by a bore. The gas enters a large gas chamber, positioned above the micro channel section, via a bore and a diffuser and leaves via the same type of conduit.

By changing the flow direction of gas and liquid streams, a co-flow and counterflow guidance is in principle possible; however, owing to the low gas velocities usually employed, this makes no practical difference [5].

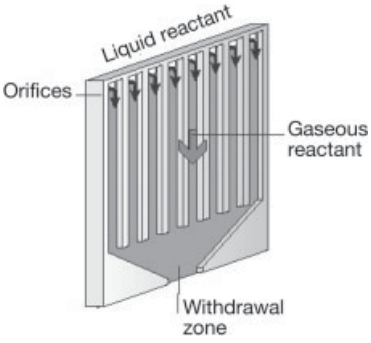

Figure 5.2 Principle of contacting liquid and gaseous reactants in a falling film micro reactor [5].

Internal heat exchange is realized by heat conduction from the microstructured reaction zone to a mini channel heat exchanger, positioned in the rear of the reaction zone [1, 3, 4]. The falling film micro reactor can be equipped, additionally, with an inspection window. This allows a visually check of the quality of film formation and identification of flow misdistribution. Furthermore, photochemical gas/liquid contacting can be carried out, given transparency of the window material for the band range of interest [6]. In some cases an inspection window made of silicon was used to allow observation of temperature changes caused by chemical reactions or physical interactions by an IR camera [4, 5].

The slit is made by μEDM; the micro channels are etched in the plate [1–3]. The gas chamber and the two diffusers are made by μEDM. The heat exchange channels are manufactured by micro milling.

Reactor type	Falling film micro reactor	Mini heat exchange channel width; depth	1500 μm; 500 μm
Housing and reaction plate material	Steel	Pressure stability	10 bar (20 bar without inspection window)
Heat exchange plate material	Copper	Temperature stability	Up to 180 °C
Outer dimensions (without connectors)	$120 \times 76 \times 40$ mm^3	Residence time	17 s (at 25 ml h^{-1})
Outer dimensions (with connectors)	$120 \times 128 \times 40$ mm^3	Interfacial area of liquid films	20 000 m^2 m^{-3} (at 25 ml h^{-1})
Number of micro channels	64	Active inner volume	100 mm^3 (per plate)
Micro reaction channel width; depth	300 μm; 100 μm	Total inner surface	1690 mm^2 (per plate)

5.1.1.2 Reactor 2 [R 2]: Continuous Two-phase Contactor with Partly Overlapping Channels

Solute transfer is performed here between immiscible phases each flowing in separate adjacent micro channels, only having as conduit a small, stable fluid interface [7]. This flow configuration is realized by having one micro channel each in two plates which are connected to a reactor sandwich. The position of these channels is so that their open channel sides do not completely overlap (as usual), but are displayed to result in partial overlap, covering more of the open area than releasing it as conduit. For this alignment, a special jig based on a mask aligner stage was applied, having a precision of positioning of ±2 μm.

The two plates were not manufactured via the same route and were not made of the same material [7]. Typically, rectangular channels in silicon are realized by sawing, whereas semi-circular channels are made in glass by wet-chemical etching. Such glass/silicon plates are joined by anodic bonding.

Several publications have referred to calculating the correct fluid layer thickness for efficient mass transfer and to determine the area of the interface sufficient to build up enough pressure to stabilize the continuous flow of the two phases and to prevent intermixing [8]. The first quantity should be below 100 μm; the channel opening should be about 20 μm.

Meanwhile, a numbered-up module was developed using the partly overlapping channels [7]; 120 single micro channels are operated here in parallel.

Reactor type	Continuous two-phase contactor with partly overlapping channels	Silicon micro channel: width; depth	Both typically 50–80 μm
Micro channels: materials	Silicon; glass	Channel opening	20 μm
Glass micro channel: diameter	35 μm	Number of micro channels per device	1–120

5.1.2 Gas/Liquid Micro Flow Dispersive Mixers Generating Slug and Annular Patterns

These devices have gas and liquid streams which merge, i.e. are fed into each other, e.g. by special dual-feed, triple-feed or multiple feed arrangements. From then, both phases are passed in the same encasing, e.g. the same micro channel. As a result of phase instability, fragmentation of the gas jet occurs under given conditions, forming a dispersion. When very small bubbles, below the characteristic length of the micro device, are generated in this way, bubbly flow is observed. More commonly, slug flow composed of alternating gas and liquid segments is achieved. At very large gas flow rates, annular flow is obtained, i.e. a thin liquid shell stream surrounding a large gas core. This pattern is similar to contacting gas and liquids in a non-dispersive manner as described in Section 5.1.1. However, the two-phase flow achieved here should be not as stable, probably creating more wavy structures, and spray phenomena (partial dispersion of the flow) are also known [9, 10]. Slug and annular flow provide very large specific interfaces for mass transfer; the latter gives even larger ones than the first.

The advantage of the dispersing principle is related to the relatively low technical expenditure to achieve dispersion, i.e. the simplicity of the concept. However, as flow patterns may change and are not known for new systems, they have to be identified, documented as flow-pattern maps and controlled. Thus, some analytical characterization has to be done in advance of the experiment. Hence inspection windows again are essential (for the first prototype; they may be eliminated later).

A slight disadvantage of the concept is phase separation, as the phases are thoroughly inter-mixed. In contrast to liquid/liquid dispersion, the gas/liquid separation should be, however, not nearly as troublesome. Another more serious drawback stems from the disperse nature of the systems involving a size distribution of the initial bubbles in the continuous liquid, which can be rather broad. By this

means, slugs of varying length may be produced. The interface is not as defined as for two-phase continuous reactors, as described in Section 5.1.1.

As a further disadvantage, it is known concerning operation in many parallel micro channels that mixed flow patterns and even drying of the channels can occur [9, 10]. This comes from phase maldistribution to the channels. To overcome this problem, first solutions for phase equipartition have been proposed recently, but so far have not been applied for the mixers described here, but instead for mini-packed reactors, having feed sections similar to the mixers [11, 12]. Nevertheless, numbering-up of dispersive-acting micro devices generally seems to be more complicated than for two-phase contactors (see Section 5.1.1).

5.1.2.1 **Reactor 3 [R 3]: Micro Bubble Column**

The micro bubble column uses dispersion of gas in a liquid stream (Figure 5.3) (and to a minor extent dispersion of liquid in a gas, as e.g. given for spray flow) [2, 3, 9]. The naming of the micro channel device stems from the prevailing flow pattern related to the guidance bubbles through a continuous liquid medium [3, 9, 10]. On the micro scale, the *slug flow* pattern, comprising bubbles of a diameter approaching that of the micro channel (Taylor bubbles) and segmented by liquid slugs, has a large range of stability; the flow pattern *bubbly flow*, which is on the macro-scale a dominating flow pattern, is also found on the micro scale, but with limited stability [9, 10]. In addition, other flow patterns known from the macro scale such as *annular-* or *spray-flow* patterns were also identified in the micro bubble column [9, 10]. The annular-flow pattern has the largest internal surface, as one uniform thin liquid film is formed. This is notably different from slug flow with co-existence of thin liquid wall-wetting films and thick liquid bubble segmenting slugs.

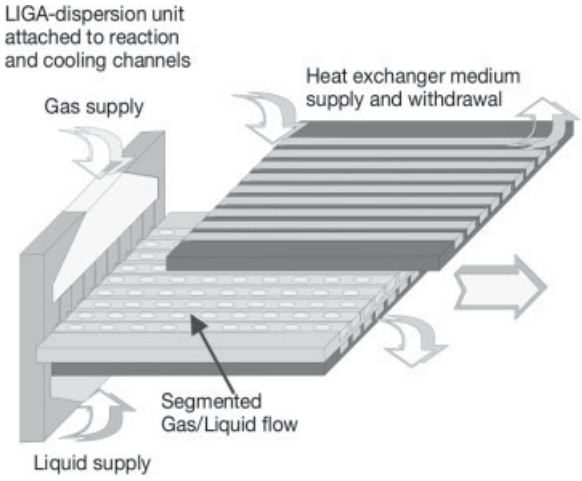

Figure 5.3 Schematic of contacting liquid and gaseous reactants in a micro bubble column [3].

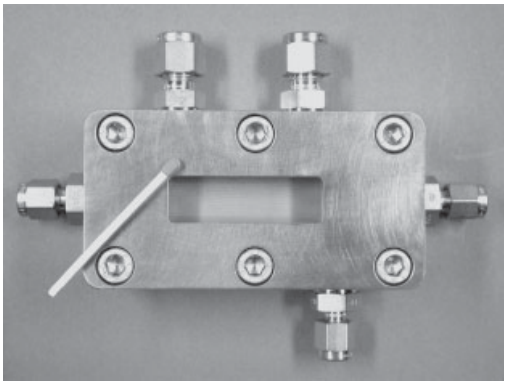

Figure 5.4 Micro bubble column (redesigned version) [IMM, unpublished].

The micro bubble column (Figure 5.4) is composed of a four-piece housing [3, 9, 10]. Two main pieces carry the micro mixing unit and the micro channel plate and are closed by two end-caps. The mixing unit comprises an interdigital feed structure with very different hydraulic diameters for gas and liquid feed. This comes from the different demands for microstructure adaptation to achieve a good pressure barrier for equipartition. Separate micro-scale gas and liquid films enter in one reaction micro channel each, which is on a separate reaction plate. By this means, a specific flow pattern is generated, determined by the process parameters, in particular the gas and liquid velocities. The gas and liquid streams merge to be removed from the micro channel section.

Reactor type	Micro bubble column	Mini heat exchange channel width; depth; length	3000 μm; 500 μm; 40 mm
Housing, heat exchange and reaction plate material	Steel	Pressure stability	30 bar
Micro mixer plate material	Nickel	Temperature stability	Up to 180 °C
Outer dimensions (without connectors)	95 × 50 × 36 mm^3	Residence time	0.14–0.56 s (at 10 ml h^{-1} liquid flow; 600–3300 ml h^{-1} gas flow)
Outer dimensions (with connectors)	143 × 102 × 36 mm^3	Interfacial area of liquid films	20 000 m^2 m^{-3} (at 25 ml h^{-1})
Number of reaction micro channels	32	Active inner volume	15.3 mm^3 (per plate)
Micro reaction channel width; depth; length	200 μm; 70 μm; 60.5 mm	Total inner surface	860 mm^2 (per plate)
Micro mixer channel width; depth; length; number (gas- and liquid site)	6, 5, 10 μm; 20 μm; 600, 2000 μm; 64; 10, 20 μm; 600 μm; 64		

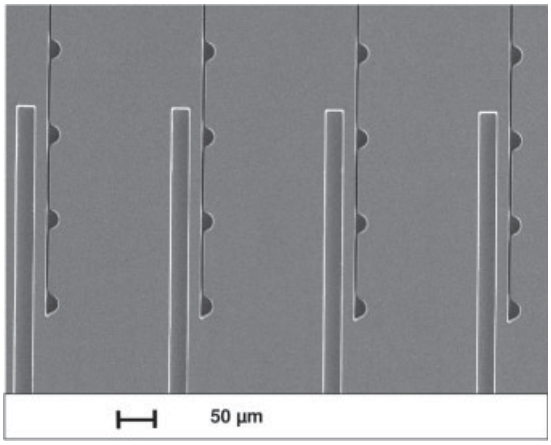

Figure 5.5 SEM of the interdigital gas and liquid feed channels [3].

The micro bubble column comprises internal cooling via heat conduction from the reaction zone to a mini channel heat exchanger [3, 9, 10]. Either two such heat exchange plates can encompass the reaction plate, or only one. In the latter case, the free position is occupied by an inspection window which allows direct observation of the quality of the flow patterns.

The micro mixing unit (Figure 5.5) is fabricated by UV lithography followed by replication via electroforming [3, 9, 10]. The reaction channels are made by wet-chemical etching. The housing is made by µEDM fabrication. The heat exchange channels are manufactured by micro milling.

Meanwhile, a redesign of the micro bubble column has been made with improved flow distribution (Figure 5.4).

5.1.2.2 **Reactor 4 [R 4]: Dual-Micro Channel Chip Reactor**

This reactor is based on two parallel micro channels that are separated by a wall. In front of the micro-channel section, one outlet hole is placed for liquid feed, followed by two holes for gas feed [13, 14]. The liquid feed enters in line with the wall long axis, while the gas feeds have the position of the two channels. Consequently, the liquid flow has to split.

The silicon chip reactor was compressed between a top plate, for direct observation of the flows, gaskets with punched holes and a base plate with all fluid connections [13, 14]. Thermocouples inserted between the two plates were located next to the micro reactor. A third inlet served for reaction quenching by introducing an inert gas such as nitrogen. Generally, heat removal is facilitated by the special reactor arrangement acting as a heat sink.

The reaction channels were made in silicon by several photolithographic steps, followed by potassium hydroxide etching [13, 14]. Silicon oxide was thermally grown over the silicon. Nickel thin films were vapor-deposited. Pyrex was anodically bonded to such a modified microstructured silicon wafer.

Reactor type	Dual-channel micro reactor	Base plate material of interfacing chip housing	Silicon stainless steel
Reactor material	Silicon; Pyrex	Gasket material	Kalrez®; hybrid Kalrez®/graphite
Micro channel: width; depth; length	435 μm × 305 μm × 20 mm (triangular cross-section)	Top plate material of interfacing chip housing	Plexiglas
Channel hydraulic diameter	224 μm	Surface-to-volume ratio of micro channels	18 000 m^2 m^{-3}
Volume of the reactor	2.7 μl	Silicon wafer: diameter; thickness	100 mm; 525 μm
Distance liquid and gas ports	3 mm	Silicon oxide layer: thickness	200–500 μm
Distance upstream end of wall to gas port	0.5 mm	Nickel layer: thickness	> 200 nm

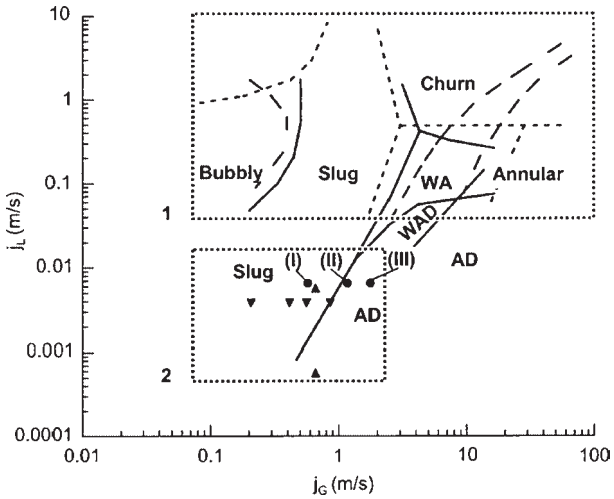

Figure 5.6 Flow pattern map for a gas/liquid flow regime in micro channels. Annular flow; wavy annular flow (WA); wavy annular-dry flow (WAD); slug flow; bubbly flow; annular-dry flow (AD). Transition lines for nitrogen/acetonitrile flows in a triangular channel (224 μm) (solid line). Transition lines for air/water flows in triangular channels (1.097 mm) (dashed lines). Region 2 presents flow conditions in the dual-channel reactor (●), with the acetonitrile/nitrogen system between the limits of channeling (I) and partially dried walls (III). Flow conditions in rectangular channels for a 32-channel reactor (150 μm) (▼) and single-channel reactor (500 μm) (▲) [13].

A flow-pattern map for gas/liquid flow (nitrogen/acetonitrile) was derived [13]. Bubbly, slug, churn and annular flows were found (Figure 5.6). In addition, wavy annular and wavy annular-dry flows were detected with a less extended stability region. Generally, the annular-flow processing was favored owing to the high specific interface and the simple concept relying on an inner gas core and surrounding liquid only.

5.1.2.3 **Reactor 5 [R 5]: Single-/Tri-channel Thin-film Micro Reactor**

This micro reactor (Figure 5.7) contains a three-plate structure forming a single micro channel and the conduits [15, 16]. The first plate is a thin frame for screw mounting and provides an opening for visual inspection of the single micro-channel section. The second plate serves as top plate shielding the micro-channel section and comprising the fluid connections. This plate also has a seal function and is transparent to allow viewing of the flow patterns in the single micro channel. The bottom plate comprises the micro channel which is made by cutting a groove in a metal block. The metal plate is highly polished to ensure gas tightness [16].

The solution containing the reactant is fed at one end of the micro channel and runs through the single micro channel for a certain passage to adapt to temperature. Then the gas stream is introduced in the flowing liquid via a second port in rectangular flow guidance [15, 16]. Thereby, the gas/liquid flow pattern is derived and the reaction initiated. After a reaction flow passage, the product mixture leaves the micro reactor via a third port.

The micro reactor was specially made for fluorination reactions. Before carrying out the fluorination reactions, passivity of the micro reactor has to be ensured by exposure of the micro channel to increasing concentrations of fluorine in nitrogen [16].

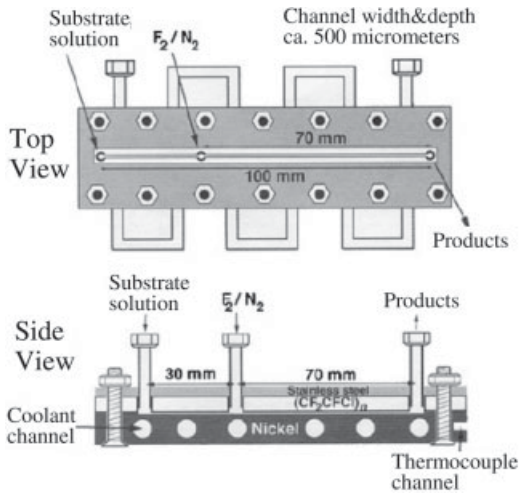

Figure 5.7 Schematic of the single-channel thin-film micro reactor [15].

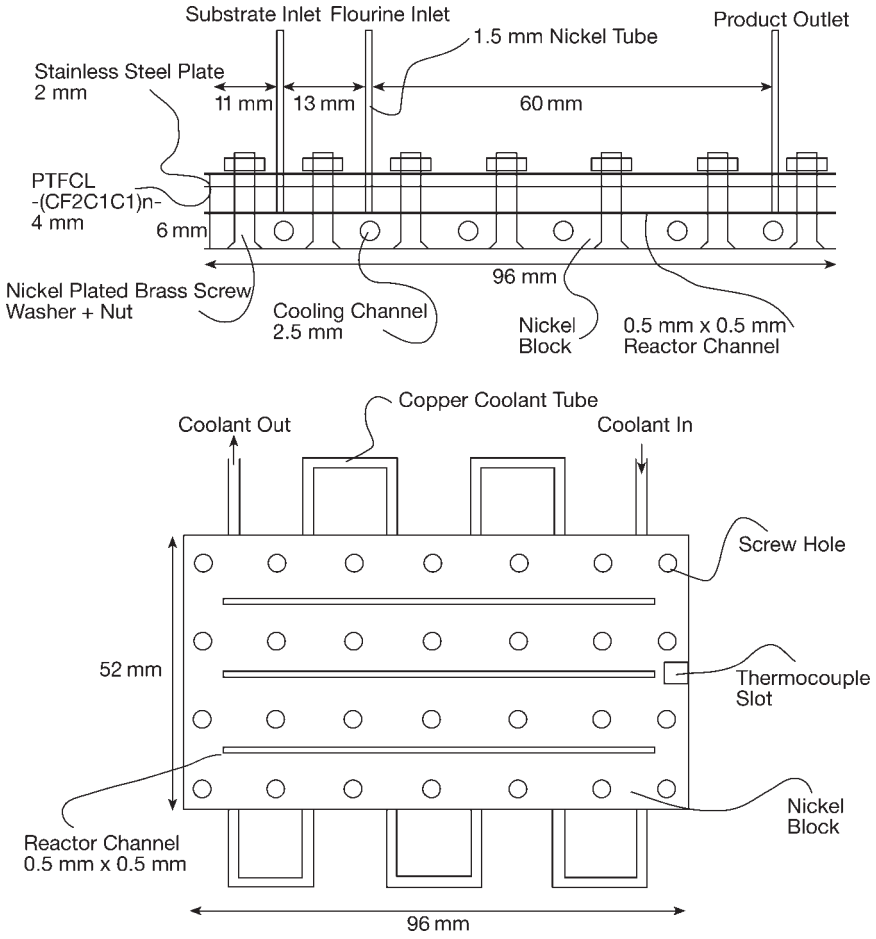

Figure 5.8 Schematic of three-micro-channel version of the single-channel micro reactor [16].

A coolant channel is guided through the metal block in a serpentine fashion [15]. Hence reactant and coolant flows are orthogonal. A thermocouple measures the temperature at the product outlet of the single-channel thin-film micro reactor.

The micro reactor was initially made as single-micro-channel version [15] and later as numbered-up (scale-out) three-micro-channel version (Figure 5.8) [16]. The data for both micro devices are given in the following.

Reactor type	Single-channel thin-film micro reactor	Bottom plate (metal block) material	Nickel (or copper)
Frame plate material	Stainless steel	Micro channel: width; depth; length	500 μm; 500 μm; 70 mm
Top plate material	Polytrifluorochloro-ethylene		

Reactor type	Three-channel thin-film micro reactor	Micro device outer dimensions	96 × 52 × 12 mm³
Frame plate material	Stainless steel	Micro channel: width; depth; length	500 µm; 500 µm; 60 mm
Top plate material	Polytrifluorochloro-ethylene	Inlet and outlet ports	Nickel tubing
Bottom plate (metal block) material	Nickel (or copper)	Nickel tubing: internal diameter; length	500 µm; 100 mm
Frame plate: thickness	2 mm	Distance liquid/gas entries	13 mm
Top plate: thickness	4 mm	Cooling channel: internal diameter	2.5 mm
Bottom plate: thickness	6 mm		

5.1.2.4 **Reactor 6 [R 6]: Modular Multi-plate-stack Reactor**

A modular reactor concept was developed to meet the typical demands of laboratory reactors, which are flexibility, easiness of handling and fast change of parameters (Figure 5.9). It is based on five different assembly groups, namely micro structured platelets, a cylindrical inner housing, two diffusers and a cylindrical outer shell with a flange [17] (see also [18, 19]). The micro structured platelets are inserted in a recess of the bottom part of the inner housing, which is a rectangular mill cut. Cylindrical tube connectors guide the flow from the reactor inlet via the diffuser to the platelet stack in the mill cut. The flange and cylindrical outer housing are bolted by six 5 mm screws and tightened via insertion of a copper gasket. The platelets are fabricated by means of thin-wire µEDM.

Even for operation of the micro reactor at 480 °C, platelet exchange can be performed rapidly, needing only 15–30 min for cooling from operational to ambient temperature [18, 19]. Heat production rates of about 30 W can be achieved without the need for external cooling [19].

A nanoporous structure on the surface of the micro channels can be realized via anodic oxidation, thereby considerably enlarging the catalyst surface [17]. Catalysts

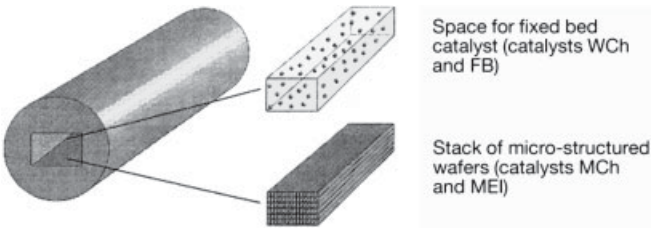

Figure 5.9 The reactor module can be equipped either with a stack of micro structured catalyst wafers or with a 'mini' fixed-bed [17].

can either be deposited by electrochemical means (e.g. palladium from $PdSO_4$ solution; 298 K; 7.5 V AC; 50 Hz; 3 min) or a chemical method can be used. The micro structured platelets were placed in 10% formalin aqueous solution, then the micro channels were exposed to a solution 200 mg of $PdCl_2$ in 40 ml of distilled water for 5 h. The $PdCl_2$ species was reduced to elemental Pd by the formalin was still present in the nanopores of the oxide layer generated one step before. This was followed by calcination. The whole procedure of impregnation was repeated several times to increase the catalyst load.

(a)

Reactor type	Multi-plate-stack in cylindrical housing	Platelet material	Aluminum
Inner housing: outer dimensions	$10 \times 10 \times 50$ mm^3	Reaction channel: width; depth; length	300 µm; 700 µm; 40 mm
Tube connectors: inner diameter	1/8 in	Total number of microstructured platelets	6
Operating pressure	3 bar		

(b)

Reactor type	Multi-plate-stack in cylindrical housing	Platelet material	Aluminum
Inner housing: outer dimensions	$10 \times 10 \times 70$ mm^3	Reaction channel: width; depth; length	300 µm; 300 µm; 70 mm
Tube connectors: inner diameter	1/8 in	Total number of microstructured platelets	140
Operating pressure	50 bar		

5.1.2.5 **Reactor 7 [R 7]: Micro-channel Reactor in Disk Housing**

Only a rough description of this micro reactor was given (Figure 5.10), not disclosing all details [20]. A pair of iron plates coated with Pd catalyst is inserted in disk-type holders. Such a supported micro channel device is encased in a housing.

Reactor type	Micro-channel reactor in disk housing	Catalyst material	Pd
Micro channel: material	Iron	Catalyst layer thickness	5 µm
Micro channel: depth	100–200 µm	Total catalyst material	20 mg
Disk holder: material	Polypropylene	Catalyst specific surface area	3.6 ± 0.4 m^2 g^{-1}
Outer casing: material	Stainless steel		

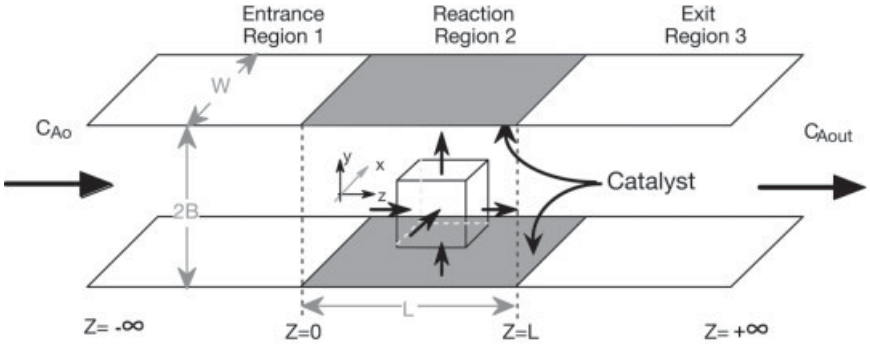

Figure 5.10 Schematic of the micro-channel reactor configuration [20].

5.1.2.6 **Reactor 8 [R 8]: Photochemical Single-channel Chip Micro Reactor**

This micro-chip reactor comprises a liquid inlet port which splits into two channels of equal passage [21]. These split channels merge with a third channel, which is connected to a second port for gas feed, in such way that the two liquid streams encompass the gas stream. This triple-stream feed section is followed by a long serpentine channel passage which ends in a third outlet port (Figure 5.11).

The microstructure is part of a bottom plate; a top plate serves as a cover [21]. Direct-write laser lithography and wet-chemical etching were employed for microfabrication of the bottom plate. Holes were drilled in the top plate to give conduits for the inlet and outlet ports. The top and bottom plates were bonded thermally.

Reactor type	Photochemical single-channel chip micro reactor	Reaction flow-through chamber: width; depth; length	150 μm; 50 μm; 50 mm
Channel material	Glass	Device outer dimensions	50 × 20 mm^2
Cover plate material	Glass		

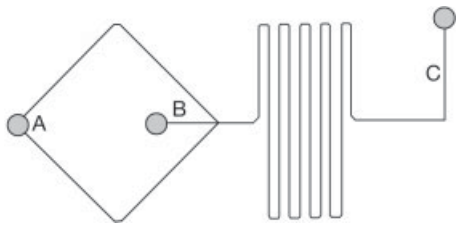

Figure 5.11 Schematic of the single-channel chip micro reactor. Divergent inlet channels (A); secondary inlet channel (B); serpentine irradiation channel (center); outlet channel (C) [21].

5.1.3 Gas/Liquid Micro Flow Dispersive Mixers Generating Bubbly Flows and Foams

These devices have gas and liquid streams which merge, i.e. are fed into each other, e.g. by special dual-feed, triple-feed or multiple-feed arrangements. Both phases are then passed in the same encasing, e.g. the same micro channel. From there, fragmentation of the gas stream occurs, forming a dispersion.

However, in contrast to the dispersive mixers forming slug and annular flow patterns, here the flow-through channel is much larger than the typical dimensions of the dispersed phase (compare with Section 5.1.2). As a result, bubbly flows and foams are the common flow patterns.

The most striking advantage of the concept is its simplicity. The micro mixers described below are commercially available, inexpensive and comparatively simple to operate.

As a further advantage, large flows are provided by these devices, even when operating with a single device. Pilot-scale operation, with one or a few micro devices, is easily feasible. Especially in the case of foam formation, parallel operation of many devices having the same flow pattern seems to be possible.

The need for analytical (flow-pattern) characterization in advance of the experiment is less than for the dispersive mixers forming slug and annular flow patterns, because the dispersion typically is formed in an attached tube. This tube is commonly made of glass and mostly of larger inner diameter. Hence visual inspection by the operator is routinely possible.

However, coalescence of the foam may occur. In aqueous systems, this may be prevented by adding surfactants to lower the surface tension. With organic solvents, this is not as facile. Hence there may be limits to applicability. For unstable gas/liquid dispersions, the micro devices described here may only be used for short-term contacting.

For systems of reduced coalescence, there is a need for phase separation, as the phases are thoroughly inter-mixed. In contrast to liquid/liquid dispersion the gas/liquid separation should be, however, much less troublesome.

Another major drawback stems from the disperse nature of the system itself involving a size distribution of the bubbles in the continuous liquid, which can be broad. The interface is not as defined as for two-phase continuous reactors, as described in Section 5.1.1. However, in the case of making foams, regular micro flow structures, such as hexagon flow, were described [22].

5.1.3.1 **Reactor 9 [R 9]: Interdigital Micro Mixer**

Interdigital micro mixers comprise feed channel arrays which lead to an alternating arrangement of feed streams generating multi-lamellae flows [23–26]. By proper shaping of the attached flow-through chamber, secondary effects can assist the diffusion mixing of the multi-lamellae. So-called triangular mixers geometrically focus the lamellae; slit-shaped mixers use jet mixing in addition to multi-lamination. In a rectangular mixer, solely multi-lamination takes place.

The interdigital feed can be fed in a counter-flow or co-flow orientation; the first principle is realized in metal/stainless-steel devices [23, 25] and the latter in glass devices [24]. Glass mixers allow observation of hydrodynamics, e.g. for process control during reaction. To prolong residence time and/or to increase temperature, tubes are usually attached to interdigital micro mixers. These comprise millimeter dimensions or below, if necessary.

For a more detailed description of interdigital micro mixers and their images see the corresponding section in Section 4.1.

Reactor type	Interdigital micro mixer	Triangular chamber: initial width; focused width; depth; focusing length; mixing length; focusing angle	3.25 mm; 500 μm; 150 μm; 8 mm; 19.4 mm; 20°
Mixer material	Metal/stainless steel; silicon/stainless steel; glass	Slit-type chamber: initial width; focused width; depth; focusing length; expansion width; expansion length; expansion angle	4.30 mm; 500 μm; 150 μm; 300 μm; 2.8 mm, 24 mm; 126.7°
Metal/silicon mixer feed channel width; depth	40 μm; 300 μm	Slit depth in steel housing	60 μm
Glass mixer feed channel width; depth	60 μm; 150 μm	Tubing attached to slit: diameter	500 μm
Type of flow-through chamber	Rectangular; triangular; slit-type	Device outer dimensions: diameter; height	20 mm; 16.5 mm
Rectangular chamber: width; depth; length	3250 μm; 150 μm; 27.4 mm		

5.1.3.2 **Reactor 10 [R 10]: Caterpillar Mini Mixer**

The caterpillar mixer acts by distributive mixing using the split–recombine approach which performs multiple splitting and recombination of liquid compartments [25–28]. A ramp-like microstructure splits the incoming flow into two parts which are lifted up and down. Thereafter, the two new streams are reshaped separately in such a way that the two new cross-sections combined restore the original one. Then, the streams are recombined, again by the lifting up and down procedure using ramps. This procedure is repeated multiple times, yielding a multilamellae flow configuration – in the ideal case.

A caterpillar steel mini mixer can be connected to conventional tubing, either stainless steel or polymeric, to prolong the residence time. The caterpillar mixer as all types of split–recombine mixers, profits from high volume flows (e.g. 100 l h^{-1} and more at moderate pressure drops) at favorable pressure drop (not exceeding 5 bar) as its internal microstructures can be held large [25–28].

For a more detailed description of the hydrodynamics of the caterpillar mixer, respective images and the performance of a second-generation caterpillar device see the corresponding section in Section 4.1.

Reactor type	Caterpillar mini mixer–tube reactor, 1st generation	Microstructure in one plate: initial depth; maximum depth	600 μm; 850 μm
Mini mixer material	Stainless steel	Mini mixer stage: length	2400 μm
Number of plates needed to form mini mixer channel	2	Number of mixing stages	8
Mini mixer channel: initial width; maximum width	1200 μm; 2400 μm	Total length of caterpillar mini mixer	19.2 mm
Mini mixer channel (both plates): initial depth; maximum depth	1200 μm; 1700 μm	Device outer dimensions	50 × 50 × 10 mm^3

5.1.3.3 **Reactor 11 [R 11]: Fork-like Chip Micro Mixer – Tube Reactor**

Central part of this reaction unit is a split–recombine chip micro mixer made of silicon based on a series of fork-like channel segments [29–33]. Standard silicon micro machining was applied to machine these segments into a silicon plate which was irreversibly joined to a silicon top plate by anodic bonding.

The fork-type chip mixer was used in connection to conventional tubes. PTFE tubing has been applied [34, 35].

Reactor type	Fork-like chip micro mixer–tube reactor	Characteristic structure of the mixing stage	'G structure'
Brand name	accoMix (μRea-4 formerly)	Inner device volume	70 μl
Micro mixer material	Silicon	Outer device dimensions	40 × 25 × 1.3 mm
Inlet channel width	1000 μm	Tube material	PTFE
Number of parallel mixing channels to which the inlet flow is distributed	9	Tube diameter	Not reported
Number of mixing stages within one mixing channel	6; 3 in top plate, 3 in bottom plate	Tube length	Not reported
Channel width; depth of micro mixer	360 μm; 250 μm (triangular-shaped)		

5.1.4
Gas/Liquid Micro Flow Packed-bed or Trickle-bed Reactors

These devices have gas and liquid streams which merge, i.e. are fed into each other, e.g. by special dual-feed, triple-feed or multiple-feed arrangements. From there, both phases are passed in the same encasing, e.g. the same micro channel.

However, in contrast to the two classes of dispersive mixers mentioned before, the attached flow-through channel contains a packed bed of particles which may carry a catalyst. This chamber is much larger than the typical dimensions of the inlet channels (e.g. compare with Section 5.1.2). The packed bed and its interstices influence the gas/liquid flow patterns, e.g. a trickle-bed operation may be established.

The most striking advantage of the concept is the resemblance of industrially applied principles for gas/liquid/solid operation. Since the packed bed may contain commercial particles, the concept is also flexible and close to the needs of applications. As a further advantage, large flows are provided, even when operating with a single device. Parallel operation of many devices has also been demonstrated [11].

Analytical (flow-pattern) characterization is more difficult as the particle bed is not transparent and covers most of the flow-through chamber. Another drawback stems from the size distribution of the particles of the catalyst bed, giving interstices which vary in typical dimensions. Here, however, today's considerable efforts in nano- and micro-material research may provide regular, mono-sized particles in the near future which will allow one to create much improved micro flow-packed beds.

5.1.4.1 **Reactor 12 [R 12]: Multiphase Packed-Bed Reactor**

The design of this micro reactor was motivated by achieving high dispersion between the liquid and gas phases and minimizing pressure drop (see especially [12, 36] for a detailed description, but also [11]). The reactor was made as two similar devices towards this end. The first version comprises a single-channel reactor with a flow-through chamber to be filled with conventional porous catalyst particles or powders. The second version has ten parallel channels, each having a staggered array of 50 μm diameter columns within to provide both catalyst support and static mixing. For the first single-channel version, a standard porous catalyst particles are inserted in a mini flow-through chamber (Figure 5.12). An inlet manifold feeds this reaction chamber. Its purpose is to introduce alternately arranged gas and liquid streams to achieve a high degree of dispersion. A filter at the outlet serves for retaining the catalyst particles (Figure 5.13). This filter is composed of regularly arranged microstructured columns. Perpendicular to the reaction channel are inlet channels for feeding the catalyst slurry.

In the multi-channel version comprising 10 packed-bed reactors (Figure 5.14), the gas flow is distributed by star-type manifolds to the 10 reaction units [11, 12].

Such a micro reactor is compressed between a cover plate, a gasket and a base plate [11]. In the cover plate a cartridge heater is inserted. The base plate provides

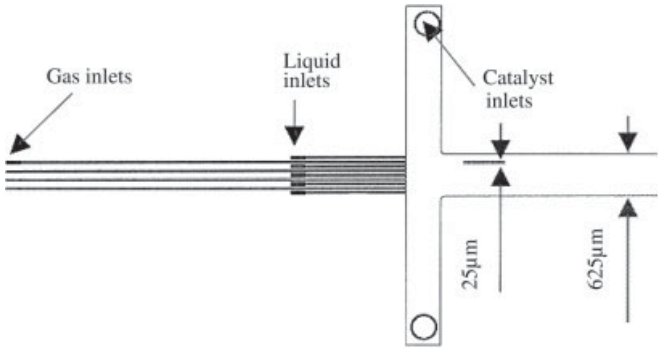

Figure 5.12 Schematic of a multiphase single-channel packed-bed reactor [36].

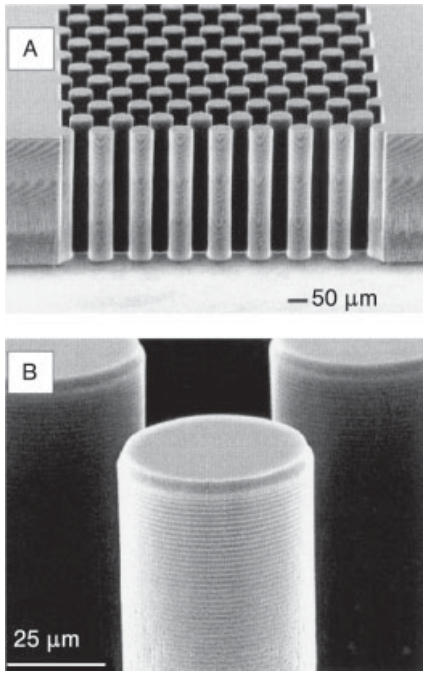

Figure 5.13 SEM images of the microstructured catalyst support in the multi-channel reactor version. Overall view (channel view) (A) and detailed view of one column (B) [12].

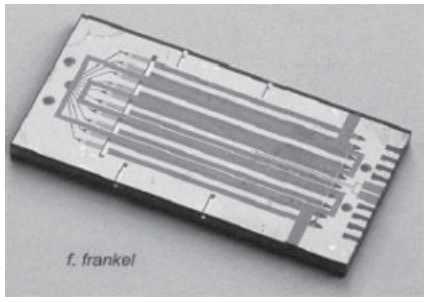

Figure 5.14 Image of a 10-channel chemical micro reactor [12].

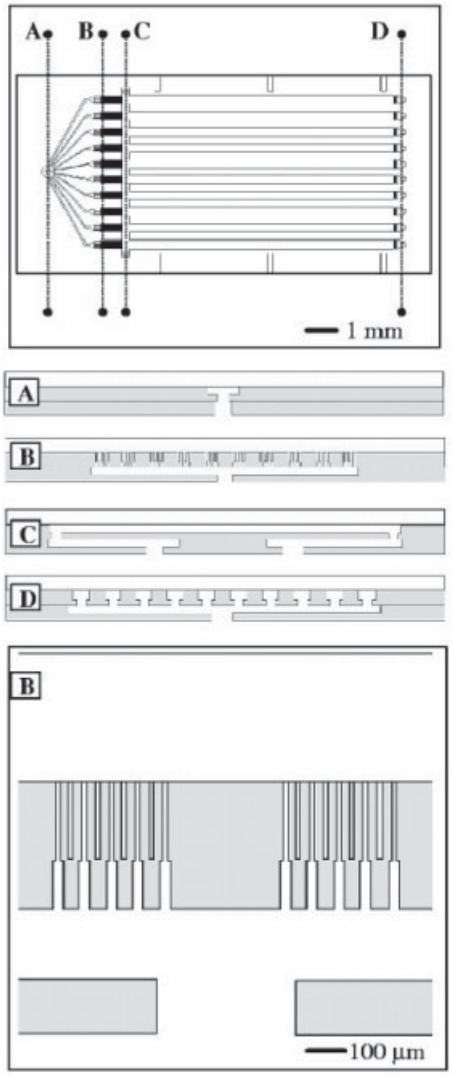

Figure 5.15 Schematic of the multiphase packed bed reactor. Gas inlet (A); liquid distributor (B); catalyst inlets (C); exit port manifold (D) [11].

conduits to the micro reactor (Figure 5.15). The outlets are standard high-pressure fittings. Thermocouples are inserted in the slurry feed channels.

Microfabrication involves multiple photolithographic and etch steps, a silicon fusion bond and an anodic bond (see especially [12] for a detailed description, but also [11]). A time-multiplexed inductively coupled plasma etch process was used for making the micro channels. The microstructured plate is covered with a Pyrex wafer by anodic bonding.

A hydrodynamic characterization of the micro reactor is given in [12]. A flow-pattern map reveals the existence of dispersed flow, annular flow, slug-dispersed

flow and slug-annular flow. The highest specific interface measured amounts to 16 000 $m^2\ m^{-3}$.

A porous surface structure (100 cm^2) in the reaction channel can be generated by an SF_6 plasma etch process with silicon nitride masking [12].

Strategies for enhanced heat control resulting in a new micro reactor design are briefly mentioned in [37].

Reactor type	Multiphase packed-bed reactor	Gasket material	Viton
Reactor material	Silicon; Pyrex	Catalyst material	Platinum on alumina
Reaction flow-through chamber: width; depth; length	625 μm; 300 μm; 20 mm	Catalyst particle diameter	50–75 μm
Gas inlet flow channels: width	25 μm	Catalyst surface area	0.57 $m^2\ g^{-1}$
Slurry inlet flow channels: width	400 μm	Catalyst weight	40 mg
Silicon substrate: diameter, thickness	100 mm; 500 μm	Catalyst loading density	0.8–1.0 g cm^{-3}
Cover plate material	Aluminum	Column diameter	50 μm
Base plate material	Stainless steel	Gap between columns	25 μm

5.2
Aromatic Electrophilic Substitution

5.2.1
Halodehydrogenation – Fluorination of Aromatic Compounds

Peer-reviewed journals: [13, 38]; proceedings: [3, 13, 14, 37, 39, 40]; sections in reviews: [26, 41–48].

5.2.1.1 Drivers for Performing Aromatic Fluorination in Micro Reactors

Aromatic fluorination certainly is one of the best candidate reactions for micro reactors. Fluorinated compounds are of high industrial interest. For instance, they find wide application as pharmaceuticals, dyes, liquid crystals and crop-protection agents [3, 13, 16, 38]; about every third drug contains a fluorine moiety. The introduction of fluorine moieties in molecules has unique effects on biological activity (see original citations in [16]).

So far, complex synthesis routes have been followed to realize these compounds, leading to a reduction in selectivity and being associated with high waste generation (see the discussion on this topic in [GL 1, below]). A direct route using the elemental material would thus be highly favorable.

This direct route demands absolutely precise temperature control because overheating of the reaction media increases radical formation [3, 13, 14, 16, 37, 38]. The number of radicals formed determines which reaction path dominates, radical or electrophilic. Another issue refers to increasing mass transfer. To utilize the potential of the extremely fast fluorination reaction, fluorine has to cross over the interface from the gas to the liquid phase. Since fluorine is hardly soluble in any organic solvent, the size of the interface becomes of special importance. In turn, control over this quantity with regard to time and space, besides heat setting, allows one to handle the delicate direct fluorination reaction. This is accompanied by a demand for precise residence time setting as the fluorination reaction is extremely fast and too long exposure to the aggressive fluorine results in secondary reactions such as multi-fluorination, C–C bond cleavage by additions, and polymerizations.

5.2.1.2 Beneficial Micro Reactor Properties for Aromatic Fluorination

The drivers for performing direct fluorinations in a micro-channel environment directly relate to the elemental advantages of micro reactors. Their large internal surface areas and interfaces facilitate mass and heat transport by building up large concentration and temperature gradients [3, 13, 14, 16, 37, 38]. Residence times can be controlled much more precisely than, e.g., in a stirred-tank reactor. Finally, the small hold-up volumes make the process safe, even if very high fluorine concentrations and hence large conversion rates are employed [16].

5.2.1.3 Aromatic Fluorinations Investigated in Micro Reactors

Gas/liquid reaction [GL 1]: Direct fluorination of toluene using elemental fluorine

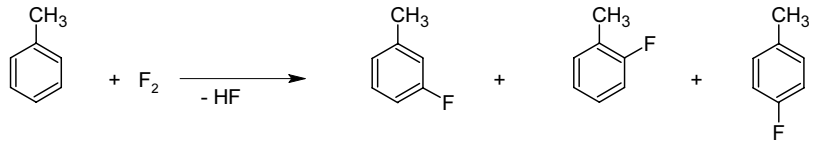

Direct fluorinations with elemental fluorine still are not feasible on an industrial scale today; they are even problematic when carried out on a laboratory-scale [49–53]. This is caused by the difficulty of sustaining the electrophilic substitution path as the latter demands process conditions, in particular isothermal operation, which can hardly be realized using conventional equipment. As a consequence, uncontrolled additions and polymerizations usually dominate over substitution, in many cases causing large heat release which may even lead to explosions.

For this reason, industrial fluorinations of aromatics are performed by other routes, mostly via the Schiemann or Halex reaction [54, 55]. As these processes are multi-step syntheses, they suffer from low total selectivity and waste production and demand high technical expenditure, i.e. a need for several pieces of apparatus.

Accordingly, for decades scientific investigations have been carried out to achieve the direct fluorination which would be attractive as a one-step synthesis alternative. Although the early reports concerned gas-phase direct fluorinations, the most relevant work in the last three decades was based on contacting fluorine gas with the aromatic compound dissolved in a liquid phase. These attempts at gas/liquid

processing focused on coping with the problem of removing the reaction heat. Mostly this was accomplished by extreme dilution or working at very low temperature or a combination of both [49–52]. By this means, it could be shown that the reaction proceeds predominantly via the electrophilic path, i.e. gives the ortho- and para-substitution patterns on the aromatic ring (see also [56]). Apart from demonstrating feasibility, the investigations could be extended to kinetic and mechanistic analysis. Using aromatic substrates of different electron density distribution, the varying reactivities could be described by the known equations in organic chemistry [51, 52].

Gas/liquid reaction 2 [GL 2]: Direct fluorination of 4-nitrotoluene using elemental fluorine

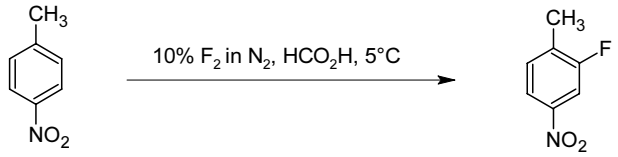

This fluorination was carried out in formic acid/acetonitrile mixtures and in acetonitrile at 5 °C [16].

5.2.1.4 Experimental Protocols

[P 1] The liquid volume flow to the micro reactor is controlled by an HPLC pump [38]. The gas flow was set by mass flow controllers. Temperature was monitored by resistance thermometers.

(a) Falling film micro reactor experiments (10% fluorine): the temperature was set to –15 to –42 °C [38] (see also [3]). The molar ratio of fluorine to toluene spans the range from 0.20 to 0.925; hence under-stochiometric fluorine contents were employed to favor mono-fluorination. The concentration of toluene in the solvent was 1.1 mol l^{-1}. As liquid volume flows 11.1 ml h^{-1}, 11.6 ml h^{-1} or 19.6 ml h^{-1} were applied. Acetonitrile or methanol was taken as solvent for the aromatic compound. In the gas phase, 10% fluorine in nitrogen was used.

(b) Falling film micro reactor experiments (> 10% fluorine): the temperature was set to –16 °C [38]. The molar ratio of fluorine to toluene spans the range from 0.40 to 2.0; hence under- and over-stochiometric fluorine contents were employed. The concentration of toluene in the solvent was 1.1 mol l^{-1}. As liquid volume flow always 19.6 ml h^{-1} was applied. Acetonitrile was taken as solvent for the aromatic compound.

(c) Micro bubble column experiments (50 × 50 μm^2 reaction channels): the temperature was set to –15 °C [38] (see also [3]). The molar ratio of fluorine to toluene spans the range from 0.20 to 0.83; hence under-stochiometric fluorine contents were employed. The concentration of toluene in the solvent was 1.1 mol l^{-1}. As liquid volume flow always 13 ml h^{-1} was applied. Acetonitrile was taken as solvent for the aromatic compound. In the gas phase, 10% fluorine in nitrogen was used. The gas volume flow was varied from 12.1 to 50.0 ml min^{-1}.

(d) Micro bubble column experiments (300 μm × 100 μm reaction channels): The temperature was set to –15 °C [38] (see also [3]). The molar ratio of fluorine to toluene spans the range from 0.20 to 0.83; hence under-stochiometric fluorine contents were employed. The concentration of toluene in the solvent was 1.1 mol l^{-1}. As liquid volume flow always 13 ml h^{-1} was applied. Acetonitrile was used as solvent for the aromatic compound. In the gas phase, 10% fluorine in nitrogen was used. The gas volume flow was varied from 12.1 ml min^{-1} to 50.0 ml min^{-1}.

(e) Laboratory bubble column experiments: the temperature was set to –17 °C. The molar ratio of fluorine to toluene spans the range from 0.40 to 1.00 [38]; hence under-stochiometric fluorine contents were employed. The concentration of toluene in the solvent was 1.1 mol l^{-1}. As liquid batch volume always 20 ml was applied. Acetonitrile or methanol was taken as solvent for the aromatic compound. In the gas phase, 10% fluorine in nitrogen was used. The gas volume flow was either 20 or 50.0 ml min^{-1}.

[P 2] A 0.1 M (and 1.0 M in one case) toluene solution was fluorinated in various solvents such as acetonitrile, methanol and octafluorotoluene using a gas mixture of 25 vol.-% fluorine in nitrogen [13]. Liquid solutions were dried with molecular sieves before use. The reactor was primed prior to operation with dry nitrogen gas and anhydrous solvent. First the reaction solution was entered, then the fluorine/nitrogen mixture. Toluene solution flow was fed by a syringe pump; the fluorine mixture was delivered by a mass-flow controller. The temperature was monitored by thermocouple. Heat removal was mainly achieved by heat conduction through the micro reactor to the top and base plate materials, acting as a heat sink.

Reactions were carried out at room temperature in the annular-dry flow regime (gas superficial velocity, 1.4 m s^{-1}; liquid superficial velocity, $5.6 \cdot 10^{-3}$ m s^{-1}) [13]. The number of fluorine equivalents (to toluene) was varied; the gas and liquid flow velocities were kept constant to maintain the same flow pattern for all experiments. Liquid products were collected in an ice-cooled round-bottomed glass flask containing sodium fluoride to trap the hydrogen fluoride. The flask is connected to a cooling condenser to recover the solvent. Samples were typically collected for 1 h. Waste gases were scrubbed in aqueous 15% potassium hydroxide solution. Samples were degassed with nitrogen and filtered before analysis.

[P 3] The reactant solutions were injected into a three-micro channel thin-film reactor via a syringe or a syringe pump [16]. The gaseous reactant was fed directly from a small cylinder by a mass-flow controller. Gas and liquid flows were started simultaneously [16]. The flow rates were so set that an annular-flow regime results, comprising a gas inner core stream surrounded by a cylindrical liquid film which wets the micro-channel's surface. This flow regime was chosen for its large specific gas/liquid interfaces and the good temperature control achievable by the thin films.

After leaving the reactant zone, the product stream enters a 0.5 in diameter FEP tube cooled by either a salt–ice bath or acetone–carbon dioxide slush bath [16]. The gas mixture was scrubbed in a soda-lime tower. Hydrogen fluoride was trapped by adding sodium fluoride to the reaction mixture or simply adding water. Then, the product solution was extracted with dichloromethane, washed with aqueous

$NaHCO_3$ solution and dried over $MgSO_4$. Thereafter, the solvent was evaporated, leaving the crude product.

A gaseous mixture of 10% fluorine in nitrogen at 10 ml min^{-1} was used [16]. The reaction was carried out at 0 °C, 5 °C and room temperature. Formic acid/acetonitrile mixtures ranging from 1 : 1 and 3 : 2 were used in addition to pure acetonitrile at single-channel flow rates of 1.0–2.0 ml h^{-1} [15]. The fluorine-to-substrate ratios were 1.7 : 1 and 3.0 : 1.

5.2.1.5 Typical Results

Conversion/selectivity/yield

[GL 1] [R 1] [P 1a] Using acetonitrile as solvent, the conversions ranged from 14 to 50% at selectivities of 33–57% [38] (see also [3]). This corresponds to yields of 5–20%. The highest yield was found for a liquid volume flow of 11.6 ml h^{-1} using a 1.1 mol l^{-1} toluene concentration at –20 °C. The fluorine/toluene molar ratio was 0.925.

Using methanol as solvent, the conversions ranged from 12 to 42% at selectivities of 9–58% [38]. This corresponds to yields of 3–14%. Hence the performance of the direct fluorination in methanol is generally worse than that in acetonitrile. The highest yield was found for a liquid volume flow of 11.1 ml h^{-1} using a 1.1 mol l^{-1} toluene concentration at –17 °C. The fluorine/toluene molar ratio was 0.925.

[GL 1] [R 1] [P 1b] Using acetonitrile as solvent, the conversions ranged from 7 to 76% at selectivities of 31–43% [38]. This corresponds to yields of 3–28%. The highest yield was found for a liquid volume flow of 19.6 ml h^{-1} using a 10% toluene/acetonitrile molar ratio at –20 °C. The fluorine/toluene molar ratio was 2.0.

[GL 1] [R 3] [P 1c] Using acetonitrile as solvent and 50 × 50 μm reaction channels, the conversions ranged from 4 to 28% at selectivities of 21–75% [38]. This corresponds to yields of 3–11%. The highest yield was found for a liquid volume flow of 13.0 ml h^{-1} and a gas volume flow of 50.0 ml h^{-1} using a 1.1 mol l^{-1} toluene concentration at –15 °C. The fluorine/toluene molar ratio was 0.54.

[GL 1] [R 3] [P 1d] Using acetonitrile as solvent and 300 × 100 μm reaction channels, the conversions ranged from 9 to 41% at selectivities of 22–28% [38]. This corresponds to yields of 2–11%. The highest yield was found for a liquid volume flow of 13.0 ml h^{-1} and a gas volume flow of 50.0 ml h^{-1} using a 1.1 mol l^{-1} toluene concentration at –15 °C. The fluorine/toluene molar ratio was 0.83.

[GL 1] [R 4] [P 2] Selectivities of up to 36% at 33% conversion were achieved using acetonitrile as solvent (1.0 fluorine-to-toluene equivalent) [13]. When including multi-fluorinated toluenes and chain-fluorinated toluenes, in addition to the monofluorinated toluenes, in the selectivity balance, the value increases to 49%. The remainder is lost in other side reactions such as additions or polymerizations.

Complete toluene conversion is achieved when using 5.0 fluorine-to-toluene equivalents [13], but at a much decreased selectivity of 11%.

The highest yield of 14% was found at 2.5 fluorine-to-toluene equivalents (58% conversion; 24% selectivity) [13]. This yield was obtained using acetonitrile as solvent; slightly lower yields were obtained for methanol (Figure 5.16). The selectivities were as high as for acetonitrile, the conversion being lower. Still lower yields (7%)

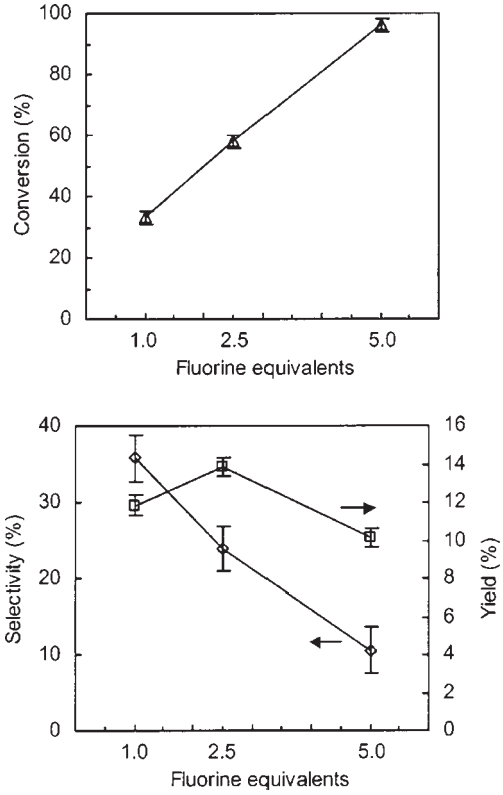

Figure 5.16 Influence of the fluorine-to-toluene equivalents (0.1 M toluene in acetonitrile) on conversion, selectivity and yield [13].

were achieved in octafluorotoluene for the same reason as for methanol, the selectivity decreasing substantially.

[GL 1] [R 4] [P 2] Conversions from 17 to 95% were achieved using methanol as solvent (1.0–10.0 fluorine-to-toluene equivalents; 0.1 M toluene; room temperature; 10 ml min^{-1} gas flow; 100 µl min^{-1} methanol) [14]. The respective selectivities ranged from 37 to 10%. Taking into account also the difluorotoluenes and trifluorotoluenes gives a selectivity of about 45%. The yields passed through a maximum at 18%.

Conversions of 35 and 52% were achieved using methanol as solvent at higher toluene concentration and with lower fluorine-to-toluene equivalents (0.5–1.0 fluorine-to-toluene equivalents; 1.0 M toluene; room temperature; 10 ml min^{-1} gas flow; 100 µl min^{-1} methanol) [14]. The respective selectivities were 20 and 17%. The yields amounted to 7 and 9%. The lower performance of the high-concentration processing compared with the more dilute 0.1 M processing is explained by a larger temperature rise leading to more pronounced radical formation causing side reactions. This is in line with calculations on heat transport for the micro reactor.

[GL 2] [R 5] [P 3] Using formic acid/acetonitrile mixtures, conversions of 44–77% and yields of 60–78% were obtained for different contents of the solvents and different flow rates [16].

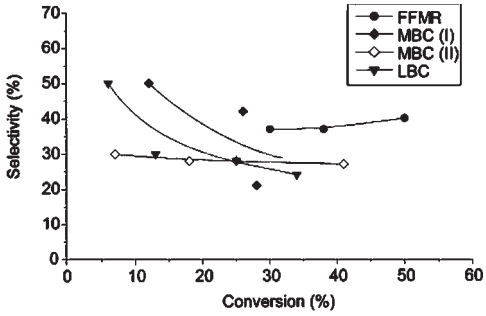

Figure 5.17 Comparison of performance of a typical laboratory column (LBC) with those of micro-reactor devices: falling film micro reactor (FFMR); micro bubble column (MBC I and MBC II) [38].

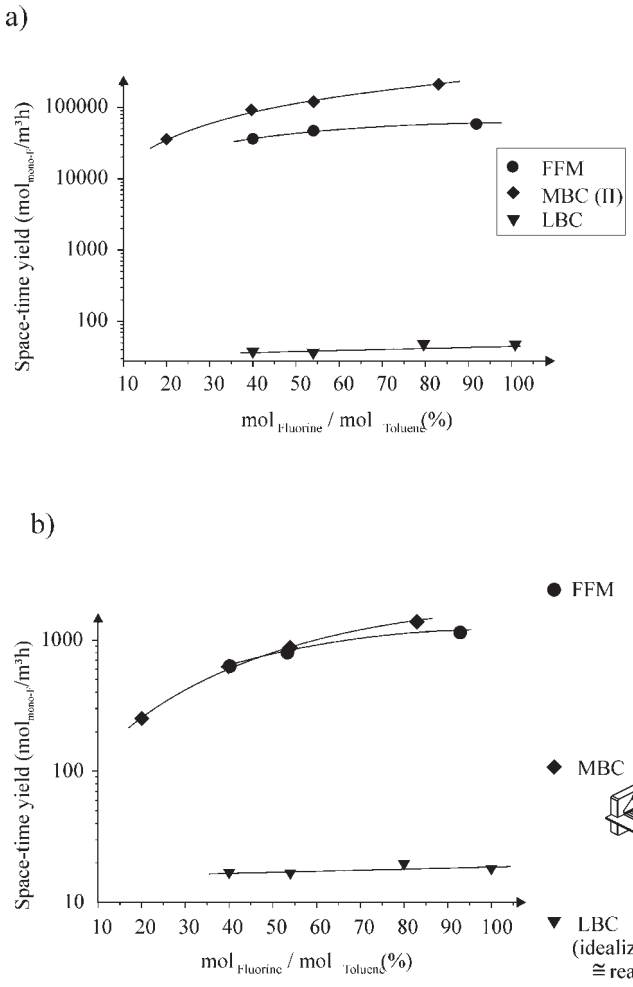

Figure 5.18 Comparison of space–time yields of direct fluorination of toluene for the falling film micro reactor (FFMR), micro bubble column (MBC) and laboratory bubble column (LBC) referred to the reaction volume (a) and referred to an idealized reactor geometry (b) [38].

Benchmarking to laboratory bubble column

[GL 1] [R 1] [R 3] [P 1e] The performance of a typical laboratory bubble column was tested and benchmarked against the micro reactors (Figure 5.17). Using acetonitrile as solvent, the conversion of the laboratory bubble column ranged from 6 to 34% at selectivities of 17–50% [3, 38]. This corresponds to yields of 2–8%. Hence the yields of the laboratory tool are lower than those of the micro reactors, mainly as a consequence of lower selectivities.

The laboratory and the micro bubble column show decreasing selectivity with increasing conversion. The falling film micro reactor shows a near-constant selectivity–conversion relationship [3, 38].

Benchmarking of the micro reactors themselves – slug flow vs. falling film

[GL 1] [R 1] [R 3] [P 1e] The falling film micro reactor has a better selectivity–conversion performance than the two micro bubble columns tested (Figure 5.18) [3, 38]. The micro bubble column with narrow channels has a better behavior at large conversion than the version with wide channels. The behavior of the falling film micro reactor and the micro bubble column with narrow channels is characterized by a nearly constant selectivity with increasing conversion, while the bubble column with wide channels shows notably decreasing selectivity with conversion (similar to the laboratory bubble column).

Ratio of *o*-, *m*- and *p*-isomers – substitution pattern

[GL 1] [R 1] [R 3] [P 1a–d] A ratio of ortho-, meta- and para-isomers for monofluorinated toluene amounting to 5 : 1 : 3 was found for the falling film micro reactor and the micro bubble column at a temperature of –16 °C [3, 38]. This is in accordance with an electrophilic substitution pathway. The relatively high amount of ortho-isomers is due to the small size of the fluorine moiety as the ortho position is amenable to steric effects.

[GL 1] [R 4] [P 2] A ratio of ortho-, meta- and para-isomers for monofluorinated toluene amounting on average to 3.5 : 1 : 2 was found in the dual-channel micro reactor at room temperature, using acetonitrile as solvent [13] (see also [14]). Ortho- and para products were the main products of the reaction mixture, unless the fluorine equivalents < 5 were used. Compared with the result cited above, the meta-isomer content was slightly higher, maybe as a consequence of using a higher reaction temperature.

Using methanol as solvent, the ratio is on average 5.5 : 1 : 2.4. Hence more products referring to an electrophilic substitution were formed [13].

An increase in toluene concentration, from 0.1 to 1.0 M, did not affect the substitution pattern when using acetonitrile as solvent [13].

Side-chain fluorination

[GL 1] [R 4] [P 2] A small amount of side-chain fluorination was reported [13]. Benzyl fluoride was formed to about the same extent as the meta isomer.

Multiple fluorination

[GL 1] [R 4] [P 2] Small amounts of difluoro- and trifluorotoluenes and also unidentified high-boiling compounds were detected [13]. Benzyl fluoride was formed to about the same extent as the meta isomer.

Space–time yield

[GL 1] [R 1] [R 3] [P 1a–d] Space–time yields higher by order of magnitude were found for the falling film micro reactor and the micro bubble column as compared with the laboratory bubble column [38]. The space–time yields for the micro reactors ranged from about 20 000 to 110 000 mol monofluorinated product $m^{-3}\,h^{-1}$. The ratio with regard to this quantity between the falling film micro reactor and the micro bubble column was about 2. The performance of the laboratory bubble column was of the order of 40–60 mol monofluorinated product $m^{-3}\,h^{-1}$.

The above-mentioned space–time yields were referred solely to the reaction volume, i.e. the micro channel volume. When defining this quantity via an idealized reactor geometry, taking into account the construction material as well, naturally the difference in space–time yield of the micro reactors from the laboratory bubble column becomes smaller. Still, the performance of the micro reactors is more than one order of magnitude better [38]. The space–time yields for the micro reactors defined in this way ranged from about 200 to 1100 mol monofluorinated product $m^{-3}\,h^{-1}$.

Fluorine-to-toluene ratio – fluorine equivalents

[GL 1] [R 1] [R 3] [P 1a–d] When the fluorine-to-toluene ratio is increased, conversion increases in a linear fashion [38]. This basically means that transport resistance would most likely not prohibit using still higher fluorine contents, thereby further possibly increasing the productivity (space–time yield) of the reactor (Figure 5.19).

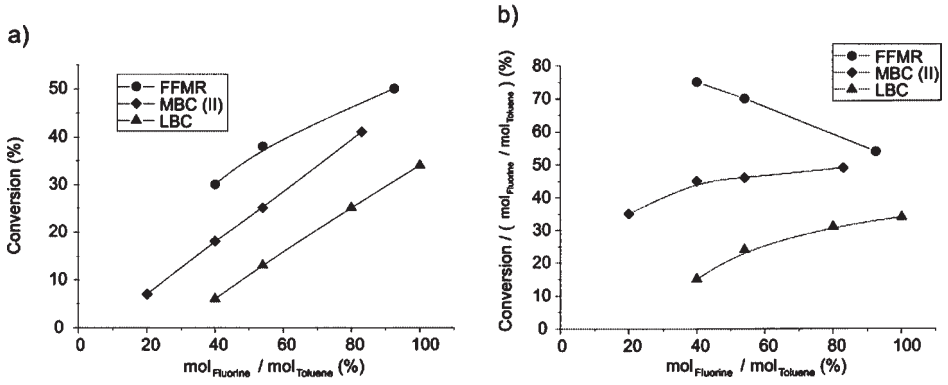

Figure 5.19 Conversion of the direct fluorination of toluene in different reactor types as a function of the molar ratio of fluorine to toluene (a) and efficiency of these reactors, defined as conversion normalized by the molar ratio of fluorine to toluene, as a function of the molar ratio of fluorine to toluene (b). Falling film micro reactor (FFMR); micro bubble column (MBC); laboratory bubble column (LBC) [38].

Content of fluorine consumed

[GL 1] [R 1] [R 3] [P 1a–d] For micro-channel processing, an analysis of the content of fluorine actually consumed as a function of the fluorine-to-toluene ratio was made [38]. The curves for two micro reactors and one laboratory bubble column do not show the same trend; a decrease of converted fluorine with increasing ratio results for the falling-film micro reactor, whereas the micro and laboratory bubble columns show increasing performance. The two micro reactors use about 50–75% of all fluorine offered, whereas the laboratory tool has an efficiency of only 15%.

[GL 1] [R 4] [P 2] A linear increase in conversion was found on increasing the number of fluorine-to-toluene equivalents (i.e. the above-mentioned ratio) from 1.0 to 5.0 [13]. By this means, the conversion increases from 33% to 96%, whereas the selectivity drops from 36% to 11% (0.1 M toluene, 25% fluorine, ambient temperature). The yield passes through a maximum.

Temperature

[GL 1] [R 1] [R 3] [P 1a–d] On increasing the temperature for micro-channel processing, conversion for the direct fluorination rises, as expected [38]. For the falling film micro reactor, conversion is increased from 15 to 30% on going from –40 to –15 °C. The selectivity varies widely between 30 and 50% without a clear tendency for this temperature range. The origin of this fluctuation is not understood.

Variation of solvent

[GL 1] [R 1] [R 3] [P 1a–d] A comparison of yield and selectivity for the direct fluorination in micro reactors when using the polar, protic solvent methanol and the polar, aprotic solvent acetonitrile was made [38]. Generally, the performance when using acetonitrile was much better; for instance, yields ranging from 20 to 28% were obtained in the falling film micro reactor. For methanol, the best yield was only 14%. This is somehow in contrast to literature findings, showing an increase in product yield with increasing solvent polarity (see citations in [38]). So far, no explanation for the differing micro channel performance has been given.

[GL 1] [R 4] [P 2] For the dual-channel micro reactor, the highest yield of 14% was found using acetonitrile (58% conversion; 24% selectivity) [13]. Slightly lower yields were obtained for methanol. The selectivities were as high as for acetonitrile, the conversion being lower. Still lower yields (7%) were achieved in octafluorotoluene for the same reason as for methanol, selectivity decreasing considerably.

[GL 1] [R 4] [P 2] A more detailed study on the methanol performance is given in [14]. Conversions from 17 to 95% were achieved (1.0–10.0 fluorine-to-toluene equivalents; 0.1 M toluene; room temperature; 10 ml min^{-1} gas flow; 100 µl min^{-1} methanol). The respective selectivities ranged from 37 to 10%. Taking into account also the difluorotoluenes and trifluorotoluenes gives a selectivity of about 45%. The yields passed through a maximum at 18%.

At higher toluene concentration and using lower fluorine-to-toluene equivalents (0.5–1.0 fluorine-to-toluene equivalents; 1.0 M toluene) [14], a lower performance is observed, which is explained by a larger temperature rise leading to more pronounced radical formation causing side reactions.

[GL 1] [R 4] [P 2] Variation of solvent affects also the substitution pattern to a certain extent [13]. A ratio of ortho-, meta- and para-isomers for mono-fluorinated toluene amounting on average to 3.5 : 1 : 2 was found in the dual-channel micro reactor at room temperature, using acetonitrile as solvent [13]. Using methanol as solvent, the ratio was on average 5.5 : 1 : 2.4. Hence more products referring to an electrophilic substitution were formed [13].

Increasing solvent polarity

[GL 2] [R 5] [P 3] By addition of formic acid, the polarity of the solvent can be enhanced, which is known to favor the electrophilic pathway. Using formic acid/acetonitrile mixtures, conversions of 44–77% and yields of 60–78% were obtained for different contents of the solvents and different flow rates [16]. The performance in pure acetonitrile was much lower (conversion, 15%; yield, 71%) and was accompanied by fouling of the micro device due to insufficient liquid reactant solubility.

Variation of residence time

[GL 1] [R 1] [R 3] [P 1a–d] In [38], only two residence times were applied, hence no large data sets were available. The yield generated for both experiments were the same, indicating that the reaction still might be much faster compared with the already short residence times in the two micro reactors.

[GL 2] [R 5] [P 3] By increasing the flow rate from 1.0 ml h^{-1} to 2.0 ml h^{-1}, the conversion increases from 44 to 53% [16]. It should be noted that the change in liquid flow rate may also have affected the flow pattern and hence the mass transfer, in addition to changing the residence time.

Residence time distribution

[GL 1] [R 1] [P 1a] The residence time distribution between the individual flows in the various micro channels on one reaction plate of a falling film micro reactor was estimated by analysing the starting wetting behavior of an acetonitrile falling film [3]. For a flow of 20 ml h^{-1}, it was found that 90% of all streams were within a 0.5 s interval for an average residence time of 17.5 s.

Experimental film thickness determination

[GL 1] [R 1] [P 1a] By autofocus laser imaging, the average position of the liquid surface in all micro channels of a reaction plate of a falling film micro reactor was determined [3]. It was found that very thin films of the order of 20–25 μm were formed for total volume flows of 20–80 ml h^{-1}. The thickness of the films in the various channels differed, but by no more than 30% on average. At high flows, e.g. > 180 ml h^{-1}, flooding of the channels occurs.

Fluorine and substrate concentration

[GL 1] [R 1] [R 3] [P 1a–d] The fluorine content in the gas phase of a falling film micro reactor was varied at 10, 25 and 50% [38]. A nearly linear increase in conversion results at constant selectivity. The substitution pattern, i.e. the ratio of ortho- to para-isomers, is strongly affected by this.

When using pure toluene instead of a dilute solution (1.1 mol l^{-1}), only a very low yield at high selectivity was found [38].

Estimation of temperature increase
[GL 1] [R 4] [P 2] A temperature rise of 0.4 K was estimated for a typical experiment in a dual-channel micro reactor based on assuming reaction rates and heat conductivity of the medium [13]. However, there are experimental indications that the real value is higher.

Corrosion
[GL 1] [R 4] [P 2] The stability of vapor-deposited protection coatings made from nickel depends on the process conditions, particularly on the concentrations of toluene and fluorine [14]. Nickel-coated silicon micro reactors were operated for several hours for the reaction conditions given. The nickel films lose to a certain extent their adhesion to the reaction channel with ongoing processing.

Safety
[GL 1] [R 1] [R 3] [P 1a–d] Fluorine contents in the gas phase of a falling film micro reactor as high as 50% could be handled safely while performing direct fluorination experiments [38].

5.3
Free Radical Substitution

5.3.1
Halodehydrogenation – Fluorination of Aliphatics and Other Species

Peer-reviewed journals: [15, 16]; sections in reviews: [26, 42–48].

5.3.1.1 Drivers for Performing Aliphatics Fluorination in Micro Reactors

Aliphatics fluorination certainly is one of the best candidate reactions for micro reactors. Fluorinated compounds are of high industrial interest. For instance, they find wide application as pharmaceuticals, dyes, liquid crystals and crop-protection agents [3, 13, 16, 38]; about every third drug contains a fluorine moiety. The introduction of fluorine moieties in molecules has unique effects on biological activity (see original citations in [16]).

So far, complex synthesis routes have been followed to realize these compounds, leading to a reduction in selectivity and being associated with high waste generation [15]. Instead, a direct route using the elemental material would be highly favorable. However, scale-up of such a direct route in conventional reactors most likely would suffer from problems with maintaining temperature control and safe handling, as fluorinations are among the most exothermic organic reactions.

Accordingly, this direct route demands absolutely precise temperature control because overheating of the reaction media increases radical formation in an un-

controlled way [3, 13, 14, 16, 37, 38]. Another issue refers to increasing mass transfer. To utilize the potential of the extremely fast fluorination reaction, fluorine has to cross over the interface from the gas to the liquid phase. Since fluorine is hardly soluble in any organic solvent, the size of the interface becomes of special importance. In turn, control over this quantity with regard to time and space, besides heat setting, allows one to handle the delicate direct fluorination reaction. This is accompanied by a demand for precise residence time setting as the fluorination reaction is extremely fast and too long exposure to the aggressive fluorine results in secondary reactions such as multi-fluorination, C–C bond cleavage, and polymerizations.

5.3.1.2 Beneficial Micro Reactor Properties for Aliphatics Fluorination

The drivers for performing direct fluorinations in a micro-channel environment directly relate to the elemental advantages of micro reactors. The large internal surface areas and interfaces facilitate mass and heat transport by building up large concentration and temperature gradients [3, 13–16, 37, 38]. Residence times can be controlled much more precisely than in a stirred-tank reactor. Finally, the small hold-up volumes make the process safe, even if very high fluorine concentrations and hence large conversion rates are employed [15, 16].

5.3.1.3 Aliphatics Fluorination Investigated in Micro Reactors

Gas/liquid reaction 3 [GL 3]: Fluorination of ethyl 3-oxobutanoate (ethyl acetoacetate) [15, 16]

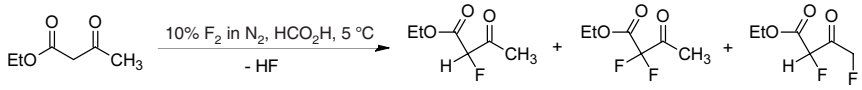

This reaction is an example of fluorination of the methylene-group of β-dicarbonyl compounds [15].

Gas/liquid reaction 4 [GL 4]: Fluorination of ethyl 2-chloro-3-oxobutanoate (ethyl 2-chloroacetoacetate) [15, 16]

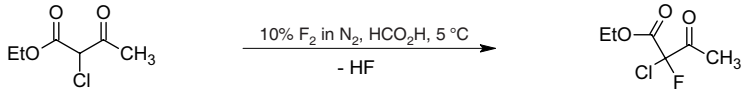

Gas/liquid reaction 5 [GL 5]: Fluorination of ethyl 2-methyl-3-oxobutanoate (ethyl-2-methylacetoacetate) [16]

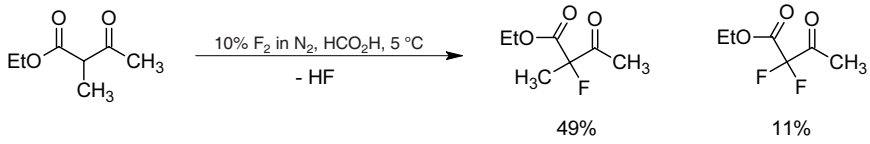

Gas/liquid reaction 6 [GL 6]: Fluorination of 3-acetyl-3,4,5-trihydrofuran-2-one [16]

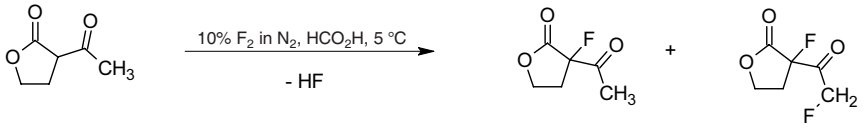

Gas/liquid reaction 7 [GL 7]: Fluorination of 2-acetylcyclohexan-one [16]

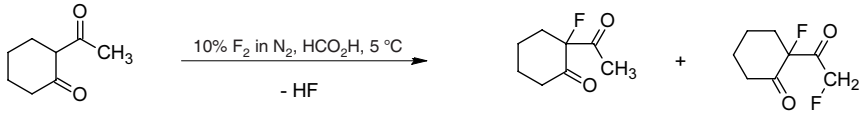

Gas/liquid reaction 8 [GL 8]: Fluorination of ethyl 2-oxocyclohexane carboxylate [16]

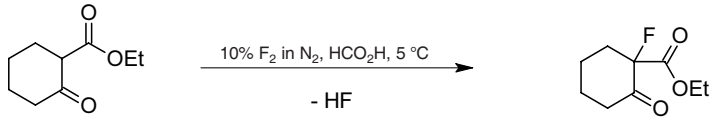

Gas/liquid reaction 9 [GL 9]: Fluorination of di(*m*-nitrophenyl) disulfide to the sulfur pentafluoride derivative [15, 16]

Gas/liquid reaction 10 [GL 10]: Fluorination of trifluorothio-*m*-nitrobenzene to the sulfur pentafluoride derivative [15, 16]

Sulfur pentafluoride derivatives are of considerable industrial interest [15]. The solubility of the di(*p*-nitrophenyl) disulfide in acetonitrile is too low to undergo a similar pathway as given in [GL 9]. Therefore, the better soluble trifluorothio-*m*-nitrobenzene was used, leading to the further fluorination of this substrate to the pentafluoro derivative as given here.

Gas/liquid reaction 11 [GL 11]: Perfluorination of tetrahydrofuran derivatives [15]

Gas/liquid reaction 12 [GL 12]: Perfluorination of cyclohexane derivatives [15]

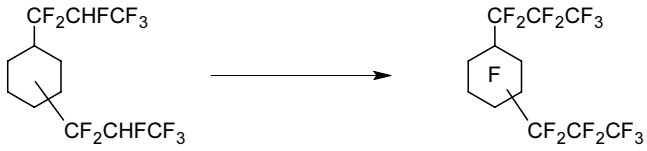

5.3.1.4 Experimental Protocols

General procedure for all experiments

The reactant solutions were injected via a syringe or a syringe pump [15, 16]. The gaseous reactant was fed directly from a small cylinder by a mass-flow controller. Gas and liquid flows were started simultaneously [16]. The flow rates were set so that an annular-flow regime results, comprising a gas inner core stream surrounded by a cylindrical liquid film which wets the micro-channel surface. This flow regime was chosen for its large specific gas/liquid interfaces and the good temperature control achievable by the thin films. Flows in the range 0.5–5.0 ml h^{-1} were used.

After leaving the reactant zone, the product stream entered a 0.5 in diameter PTFE tube cooled either by salt–ice bath or acetone–carbon dioxide slush bath [15, 16]. The gas mixture was scrubbed in a soda-lime tower. Hydrogen fluoride was trapped by adding sodium fluoride to the reaction mixture or simply adding water. Then, the product solution was extracted with dichloromethane, washed with aqueous $NaHCO_3$ solution and dried over $MgSO_4$. Thereafter, the solvent was evaporated, leaving the crude product.

[P 4] 10% fluorine in nitrogen at 10 ml min^{-1}; 5 °C; formic acid as solvent at 0.5 ml h^{-1} [15].

[P 5] 10% fluorine in nitrogen at 10 ml min^{-1}; 5 °C; formic acid as solvent at 0.25 ml h^{-1} [15].

[P 6] 10% fluorine in nitrogen at 10 ml min^{-1}; room temperature; acetonitrile as solvent at 0.5 ml h^{-1} [15].

[P 7] 50% fluorine in nitrogen at 15 ml min^{-1}; room temperature; no solvent; 0.5 ml h^{-1} liquid flow [15].

[P 8] 50% fluorine in nitrogen at 15 ml min^{-1}; room temperature, then 280 °C; no solvent; 0.5 ml h^{-1} liquid flow [15].

[P 9] 20% fluorine in nitrogen at 20 ml min^{-1}; room temperature; no solvent; 0.5 ml h^{-1} liquid flow [15].

[P 10] 50% fluorine in nitrogen at 10 ml min^{-1}; room temperature, then 50 °C; no solvent; 0.5 ml h^{-1} liquid flow [15].

[P 11] 50% fluorine in nitrogen at 15 ml min^{-1}; room temperature, then 280 °C; no solvent; 0.5 ml h^{-1} liquid flow [15].

5.3.1.5 Typical Results

Conversion/selectivity/yield

[GL 3] [R 5] [P 4] Yields of 73/71% were achieved at 99/98% conversion [15, 16], respectively. The amount and nature of difluorinated products were also specified in [16].

[GL 4] [R 5] [P 5] A yield of 62% was achieved at 90% conversion [15]. The amount and nature of difluorinated products was also specified in [16]. Besides this performance in single micro-channels, conversion and yield for a three-micro-channel reactor given [16].

[GL 5] [R 5] [P 5] A yield of 49% was achieved at 52% conversion [15]. The amount and nature of difluorinated products was also specified in [16].

[GL 6] [R 5] [P 5] A yield of 95% was achieved at 66% conversion [15]. The amount and nature of difluorinated products was also specified in [16].

[GL 7] [R 5] [P 5] A yield of 78% was achieved at 93% conversion [15]. The amount and nature of difluorinated products was also specified in [16].

[GL 8] [R 5] [P 5] A yield of 76% was achieved at 86% conversion [15].

[GL 9] [R 5] [P 6] A yield of 75% was achieved [15].

[GL 10] [R 5] [P 6] A yield of 44% was achieved [15]. An improved yield of 56% is reported in [16].

[GL 11] [R 5] [P 7] [P 8] A yield of 91% of the perfluorinated product was achieved (52% recovery) when using an additional heating stage to complete the reaction [15].

[GL 12] [R 5] [P 9] [P 10] [P 11] A yield of 70% of the perfluorinated product was achieved (82% recovery) when using an additional heating stage to complete the reaction [15].

Catalytic effect of metal surface

[GL 3] [R 5] [P 4] A catalytic effect of the fluorinated metal surface of the micro channel was clearly determined [15].

[GL 12] [R 5] [P 9] [P 10] [P 11] A high yield of 70% of the perfluorinated product was achieved without using the conventionally used cobalt trifluoride [15].

See also the next section for the importance of the surface on enol formation.

Importance of enol formation for β-keto ester fluorination

[GL 4] [R 5] [P 5] The rate of the fluorination of β-keto esters is usually correlated with the enol concentration or the rate of enol formation as this species is actually fluorinated [15, 16]. For the fluorination of ethyl 2-chloroacetoacetate in a micro reactor, much higher yields were found as expected from such relationships and as compared with conventional batch processing which has only low conversion. Obviously, the fluorinated metal surface of the micro channel promotes the enol formation.

Temperature

[GL 12] [R 5] [P 9] [P 10] [P 11] Significantly lower temperature can be used to achieve a yield of the perfluorinated product as high as when employing the conventionally used cobalt trifluoride process with traditional reactors [15].

Single- vs. three-micro-channel processing

[GL 3] [GL 4] [GL 5] [GL 6] [GL 7] [R 5] [P 5] No clear difference in the performance of a single-channel micro reactor and a numbered-up three-channel micro reactor was detected [16]. However, many differences in the results were found which were

probably due to fluctuations in the micro-channel hydrodynamics in general, rather than being a consequence of the numbering-up (e.g. due to flow maldistribution). Overall, this means that, despite partly unstable processes, the numbering-up concept was successful, i.e. no performance was lost during scale-out.

Safety

[GL 12] [R 5] [P 9] [P 10] [P 11] Hazardous perfluorination processes with high yield can be carried out safely in micro reactors [15].

5.3.2 Halodehydrogenation – Chlorination of Alkanes

Peer-reviewed journals: [6]; proceedings: [40]; sections in reviews: [47].

5.3.2.1 Drivers for Performing Alkane Chlorination in Micro Reactors

Side-chain photochlorination of toluene isocyanates yields important industrial intermediates for polyurethane synthesis, one of the most important classes of polymers [6]. The motivation for micro-channel processing stems mainly from enhancing the performance of the photo process. Illuminated thin liquid layers should have much higher photon efficiency (quantum yield) than given for conventional processing. In turn, this may lead to the use of low-intensity light sources and considerably decrease the energy consumption for a photolytic process [6] (see also [21]).

Owing to the planar layer structure of most micro reactors, uniform illumination is yielded in addition, which can be maintained on increasing throughput by numbering-up [6]. Here, the individual reaction units are assembled in parallel again on a plane, but a larger one.

5.3.2.2 Beneficial Micro Reactor Properties for Alkane Chlorination

Considering the drivers outlined above, the relevant micro reactor property is the capability to provide thin liquid layers. This is advantageous both for increasing the photon efficiency (quantum yield) and for the mass transfer across the gas/liquid interface [6]. As another result, the residence time may be considerably reduced, thereby decreasing side and follow-up reactions. Overheating as a consequence of using high-intensity light sources at low efficiency can be avoided, thus reducing thermally induced side reactions. The use of low-intensity light sources may change the technical expenditure needed for photoreactions and result in a completely different cost-investment scenario when building a new plant.

5.3.2.3 Alkane Chlorination Investigated in Micro Reactors

Gas/liquid reaction 13 [GL 13]: Photochlorination of toluene-2,4-diisocyanate

Chlorine molecules are cleaved at high temperatures by photoinduced radical formation. By this means, a gas/liquid reaction can be performed in the side chain of alkyl aromatics quite selectively. The electrophilic ring substitution, instead, is favored using Lewis catalysts in polar solvents at low temperature.

Via such a gas/liquid reaction, toluene-2,4-diisocyanate reacts with chlorine to give 1-chloromethyl-2,4-diisocyanatobenzene [6]. As a ring-substituted side product, toluene-5-chloro-2,4-diisocyanate is formed in minor quantities.

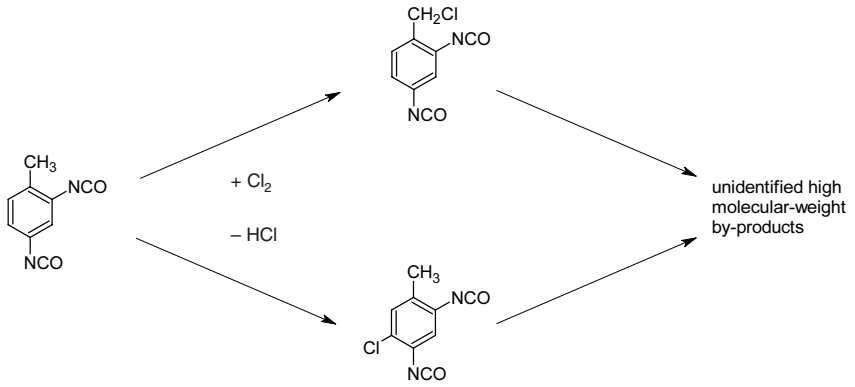

Typically, the reaction mechanism proceeds as follows [6]. By photoreaction, two chlorine radicals are formed. These radicals react with the alkyl aromatic to yield a corresponding benzyl radical. This radical, in turn, breaks off the chlorine moiety to yield a new chlorine radical and is substituted by the other chlorine, giving the final product. Too many chlorine radicals lead to recombination or undesired secondary reactions. Furthermore, metallic impurities in micro reactors can act as Lewis catalysts, promoting ring substitution. Friedel–Crafts catalyst such as $FeCl_3$ may induce the formation of resin-like products.

5.3.2.4 **Experimental Protocols**

[P 12] A falling film micro reactor was applied for generating thin liquid films [6]. A reaction plate with 32 micro channels of channel width, depth and length of 600 μm, 300 μm and 66 mm, respectively, was used. Reaction plates made of pure nickel and iron were employed. The micro device was equipped with a quartz window transparent for the wavelength desired. A 1000 W xenon lamp was located in front of the window. The spectrum provided ranges from 190 to 2500 nm; the maximum intensity of the lamp is given at about 800 nm.

For the range of flows applied (0.12, 0.23, 0.38 and 0.57 ml min^{-1}), the average film thickness was calculated to be 21–36 μm [6]. The corresponding residence times and specific interfacial areas amount to 4.8–13.7 s and 28 000–48 000 $m^2\ m^{-3}$, respectively. A pump was used for liquid feed. The gas flow was controlled by a mass-flow controller, ranging from 14–56 ml min^{-1}. This provides an equimolar ratio of toluene-2,4-diisocyanate and chlorine. A solution of 0.1 mol of toluene-2,4-diisocyanate (14.4 ml) in 30 ml of tetrachloroethane was used (concentration: 3.3 mol l^{-1}). The reaction temperature of 130 °C was achieved by guiding a heating medium through the mini-channel heat exchanger of the device, heating up the back side of the reaction plate. Temperatures were controlled at the product inlet and outlet. The product stream was actively removed by another liquid pump to avoid overfilling of the outlet bore, which may affect the falling film.

5.3.2.5 Typical Results

Conversion/selectivity/yield – by-product analysis – benchmarking

[GL 13] [R 1] [P 12] Conversions from 30 to 81% at selectivities from 79 to 67% and yields from 24 to 54%, were found when using a falling film micro reactor (4.8–13.7 s; 130 °C) [6].

A selectivity–conversion plot for the product, the ring-substituted by-product and other, so far unidentified, by-products is given in [6] (Figure 5.22). While the content of the ring-substituted product decreased with increasing conversion (12–5%), the other by-products were formed in much larger amount (8–29%). This also indicates that the other by-products are formed by consecutive reactions at longer residence times.

Control experiments in a batch reactor (30 ml reaction volume) at a 30 min reaction time resulted in a conversion of 65% at 45% selectivity, hence having a selectivity which is higher by about a factor of 2 [6]. Interestingly, the selectivity of the ring-substituted by-product is 54%, different from the more dominant resin-formation in the micro reactor (Figure 5.20). The superior performance of the micro reactor is explained by the better photon yield stemming from the use of very thin liquid films. The low penetration of light in the conventional batch reactor generates largely reaction conditions which are not photoinduced, hence favoring ring chlorination.

Flow rate

[GL 13] [R 1] [P 12] When using lower flow rates, conversion is increased as a consequence of both increasing residence time and decreasing film thickness [6]. Reducing the flow rate from 0.57 ml min^{-1} to 0.12 ml min^{-1} leads to an increase in conversion from 30 to 81%. Selectivity is nearly unaffected, with the exception of the smallest flow rate.

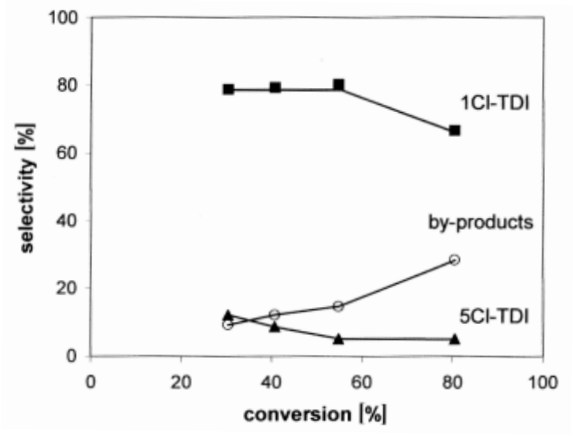

Figure 5.20 Selectivities of main and side product as a function of toluene-2,4-diisocyanate conversion when using a nickel-plate equipped micro reactor (Reactant ratio 1 : 1; 130 °C) [6].

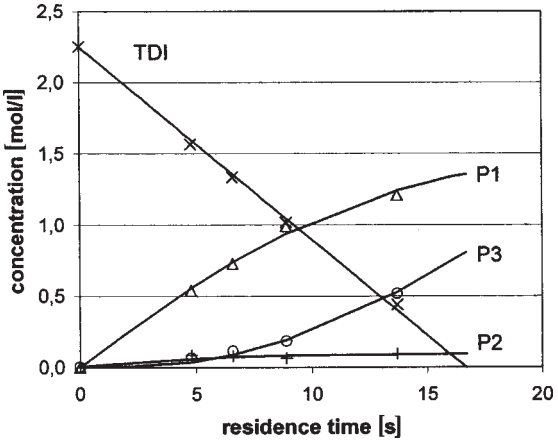

Figure 5.21 Comparison of reaction product concentrations (symbols) and model (solid line) as a function of residence time given in [6]. Toluene-2,4-diisocyanate (TDI); 1-chloromethyl-2,4-diisocyanatobenzene (P_1); toluene-5-chloro-2,4-diisocyanate (P_2); high-molecular-weight consecutive products (P_3) [6].

Residence time

[GL 13] [R 1] [P 12] As a function of residence time, conversion increases linearly from 30 to 81% at selectivities from 79 to 67% [6]. The associated yield increase is non-linear and seems to approach a plateau (Figure 5.21). Hence residence times much larger than 14 s are not suited to increase reactor performance.

Use of iron plate – formation of Lewis acids

[GL 13] [R 1] [P 12] By using an iron plate (instead of a non-active nickel plate), the impact of Lewis acid formation on the reaction course could be tested [6] (Figure 5.21). As a result, the selectivity to the target product decreases drastically, e.g. at a conversion of 80% it decreases to 50% (from 67% using a nickel plate). Interestingly, the content of ring-substituted isomer is not enhanced (actually it is reduced), but probably resin-type condensation products are formed instead yielding the product (Figure 5.22).

Space–time yield – benchmarking

[GL 13] [R 1] [P 12] By using a nickel plate, space–time yields up to 401 mol l^{-1} h^{-1} were achieved in the falling film micro reactor [6]. Control experiments in a batch reactor at a 30 min reaction time resulted in a space–time yield of only 1.3 mol l^{-1} h^{-1}, hence orders of magnitude smaller. By using an iron plate, space–time yields up to 346 mol l^{-1} h^{-1} were achieved in the falling film micro reactor.

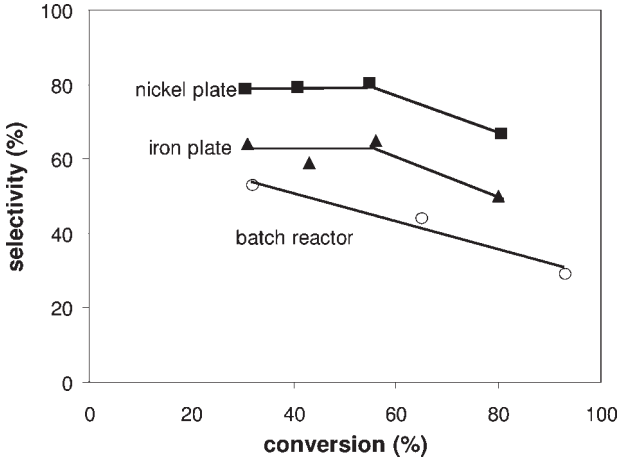

Figure 5.22 Influence of different reactor materials on selectivity for 1-chloromethyl-2,4-diisocyanatobenzene and toluene-2,4-diisocyanate conversion [6].

Kinetics – reaction modeling

[GL 13] [R 1] [P 12] Using a reaction model assuming plug-flow behavior and taking into account consecutive elemental reactions, the dynamic development of the species' concentrations can be predicted [6]. This fits well with experimental data when a reaction order of 0.1 is used (Figure 5.23). This is in contrast to comparable literature approaches relying on a first-order reaction with respect to chlorine and toluene. Also, a selectivity–conversion plot can be drawn for the target product, by-product and consecutive product.

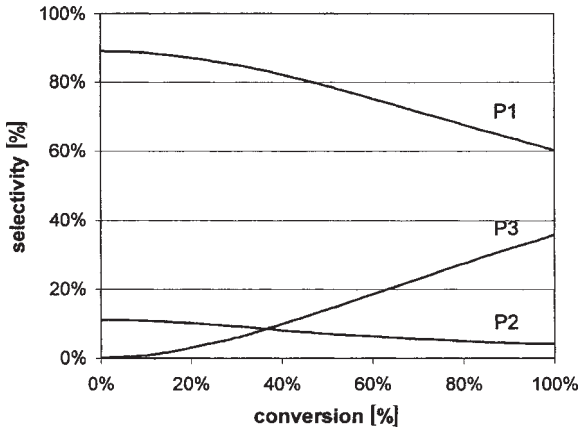

Figure 5.23 Simulated selectivity versus conversion of toluene-2,4-diisocyanate (TDI). P_1 is the target product 1-chloromethyl-2,4 diisocyanatobenzene; P_2 is the side-product 5-toluene-5-chloro-2,4-diisicyanate; P_3 represents high-molecular-weight consecutive products [6].

5.3.3 Halodehydrogenation – Chlorination of α-Keto Compounds

Patents: [57]; sections in reviews: [47].

5.3.3.1 Drivers for Performing Chlorination of α-Keto Compounds in Micro Reactors

The motivation of an industrial development was to increase selectivity for monochlorination of acetic acid to give chloroacetic acid [57]. This product is amenable under suitable reaction conditions by further chlorination to give dichloroacetic acid by consecutive reaction. The removal of this impurity is not simple, but rather demands laborious and costly separation. Either crystallization has to be performed with high technical expenditure or an expensive hydrogen reduction at a Pd catalyst is needed.

5.3.3.2 Beneficial Micro Reactor Properties for Chlorination of of α-Keto Compounds

The consecutive reaction will be triggered by too long exposure of already chlorinated product in an environment with a high density of chlorine radicals. Accordingly, controls over residence time, concentration profiles and efficient heat transfer have the potential to cope with such a problem.

5.3.3.3 Chlorination of of α-Keto Compounds Investigated in Micro Reactors

Gas/liquid reaction 14 [GL 14]: Chlorination of acetic acid

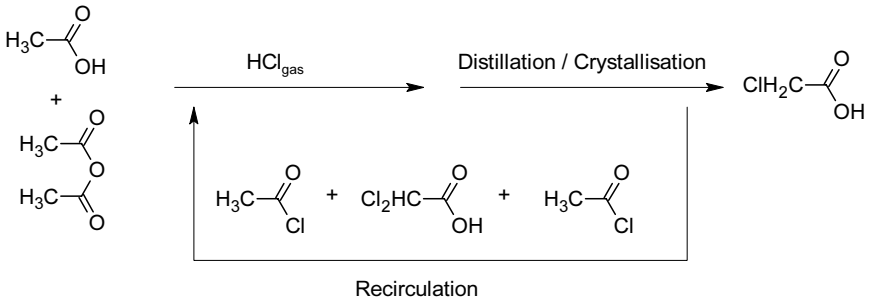

This process is carried out on an industrial scale in bubble columns [57]. Acetic acid and acetic anhydride are fed together with a recycle solution composed of acetic acid, acetyl chloride, monochloroacetic acid, dichloroacetic acid and hydrogen chloride. Under these conditions, acetic anhydride and hydrogen chloride give acetyl chloride spontaneously.

This mixture is fed into bubble columns and contacted with chlorine gas at 3.5 bar and 115–145 °C [57]. A typical reaction mixture has a composition of 38.5% acetic acid, 11.5% acetic anhydride and 50% chlorine gas. The crude product is first purified by distillation. Thereafter, either crystallization or hydrogen reduction at a Pd catalyst is conducted to separate the monochlorinated from the dichlorinated product.

5.3.3.4 Experimental Protocols

[P 13] Micro channels of 1500 μm width and 300 μm depth, separated by fins of 150 μm width, were employed [57].

Acetic acid and 10, 15, or 20% acetyl chloride were fed as a mixture into a modified falling film micro reactor (also termed micro capillary reactor in [57]) at a massflow rate of 45 g min^{-1} and a temperature of 180 or 190 °C [57]. Chlorine gas was fed at 5 or 6 bar in co-flow mode so that a residual content of only 0.1% resulted after reaction. The liquid product was separated from gaseous contents in a settler and collected. By exposure to water, acetyl chloride and acetic anhydride were converted to the acid. The hydrogen chloride released was removed.

5.3.3.5 Typical Results

Yield/selectivity/conversion – benchmarking to industrial bubble-column processing

[GL 14] [R 1] [P 13]* A yield of 85% was obtained by micro flow processing similarly to large-scale bubble column processing [57]. Selectivity was much better since less than 0.05% dichloroacetic acid was formed, whereas conventional processing typically gives 3.5%.

[R 1*] is a modified [R 1] micro device, the exact design of which has not been disclosed.

Numbering-up – benchmarking to industrial bubble-column processing

[GL 14] [R 1] [P 13]* Three falling-film units were operated in parallel in one device [57]. A yield of 85% and < 0.1% dichloroacetic acid resulted, exceeding the performance of conventional processing.

Temperature/pressure

[GL 14] [R 1] [P 13]* Increasing both temperature and pressure slightly increases the yield from 85% to 90% [57]. The content of dichloroacetic acid was below 0.05%.

5.3.4 Hydrodehalogenation – Dechlorination of Aromatics

Proceedings: [20].

5.3.4.1 Drivers for Performing Dechlorination of Aromatics in Micro Reactors

Micro reactors may be used for the removal of chlorinated organic compounds such as found in stockpiles of mixed waste [20]. On-site use of micro reactors may benefit from eliminating the need for waste transport, reduces the risk of exposure, could have lower investment and processing costs and may reduce the generation of secondary waste. These advantages seem to be clear, but so far there is no documentation in the literature giving experimental evidence.

5.3.4.2 Beneficial Micro Reactor Properties for Dechlorination of Aromatics

The above-mentioned drivers stem from the fact that micro reactors may be constructed light-weight and so are potentially mobile [20]. This holds particularly when integration of many components into one system can be performed. In addition, micro reactors can generally have high mass transfer efficiency, especially when

considering multi-phase processes as they provide large specific interfaces. This is needed when small-volume reactors are required to process large volumes of reactant solutions.

Reductions of investment and processing costs are general benefits that have been predicted for a long time; so far, this has not yet been demonstrated. This is strongly coupled with an onset of mass fabrication, proposed to have similar benefits as for microelectronics, which has not happened so far.

5.3.4.3 Dechlorination of Aromatics Investigated in Micro Reactors

Gas/liquid reaction 15 [GL 15]: Dechlorination of *p*-chlorophenol to phenol

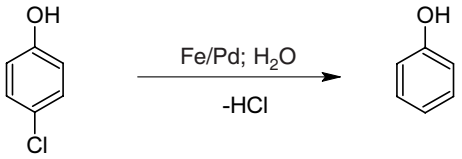

This process involves a series of reactions, including dissolution, hydrogen reactions and chlorine withdrawal [20]. The second type of reactions include reduction of protons at the catalyst by electron transfer yielding hydrogen radicals that are consumed by reaction or give elemental hydrogen otherwise.

As catalyst, a Pd/Fe system is used, having finely dispersed Pd clusters (< 1 μm) on the Fe surface [20] (see also original citations in [20]). A considerable portion of the surface remains uncovered, exposing Fe for reaction.

5.3.4.4 Experimental Protocols

[P 14] A solution containing *p*-chlorophenol was fed from a 250 ml flask to the micro reactor by a syringe pump [20]. Flow rates from 10 to 65 ml min^{-1} were applied. The reaction temperature was set to either 20 or 40 °C.

The micro reactor consisted of a pair of iron plates coated with Pd catalyst placed on disk-type polypropylene holders [20]. This micro channel device was encased in a stainless-steel housing. The thickness of the catalyst layer was approximately 5.0 μm; 10 mg catalyst was deposited per plate, so giving 20 mg in total. The specific surface area of the catalyst was 3.6 ± 0.4 $m^2\ g^{-1}$.

5.3.4.5 Typical Results

Dynamic behavior of catalyst

[GL 15] [R 7] [P 14] During a 24 h period, only minimal deactivation could be detected [20]. Only about 10–15% of the *p*-chlorophenol was converted.

Reaction rates

[GL 15] [R 7] [P 14] The reaction rate constant K''_w ranged from $3.15 \cdot 10^{-7}$ to $7.86 \cdot 10^{-7}\ m_{reactor}\ s^{-1}$ depending on the flow rate (0.10–0.63 ml min^{-1}), channel depth (100, 200 μm) and temperature (20, 40 °C) [20]. Only about 10–15% of the *p*-chlorophenol was converted.